Brain Advance Access published June 24, 2016

doi:10.1093/brain/aww153 BRAIN 2016: Page 1 of 12 | 1

BRAIN
A JOURNAL OF NEUROLOGY

NRSN1 associated grey matter volume of the visual word form area reveals dyslexia before school

Michael A. Skeide,[1] Indra Kraft,[1] Bent Müller,[2] Gesa Schaadt,[1,3] Nicole E. Neef,[1] Jens Brauer,[1] Arndt Wilcke,[2] Holger Kirsten,[2,4,5] Johannes Boltze[2,6] and Angela D. Friederici[1]

Literacy learning depends on the flexibility of the human brain to reconfigure itself in response to environmental influences. At the same time, literacy and disorders of literacy acquisition are heritable and thus to some degree genetically predetermined. Here we used a multivariate non-parametric genetic model to relate literacy-associated genetic variants to grey and white matter volumes derived by voxel-based morphometry in a cohort of 141 children. Subsequently, a sample of 34 children attending grades 4 to 8, and another sample of 20 children, longitudinally followed from kindergarten to first grade, were classified as dyslexics and controls using linear binary support vector machines. The *NRSN1*-associated grey matter volume of the 'visual word form area' achieved a classification accuracy of ~ 73% in literacy-experienced students and distinguished between later dyslexic individuals and controls with an accuracy of 75% at kindergarten age. These findings suggest that the cortical plasticity of a region vital for literacy might be genetically modulated, thereby potentially preconstraining literacy outcome. Accordingly, these results could pave the way for identifying and treating the most common learning disorder before it manifests itself in school.

1 Department of Neuropsychology, Max Planck Institute for Human Cognitive and Brain Sciences, Stephanstraße 1a, 04103 Leipzig, Germany
2 Cognitive Genetics Unit, Department of Cell Therapy, Fraunhofer Institute for Cell Therapy and Immunology, Perlickstraße 1, 04103 Leipzig, Germany
3 Department of Psychology, Humboldt-Universität zu Berlin, Rudower Chaussee 18, 12489 Berlin, Germany
4 Institute for Medical Informatics, Statistics and Epidemiology, Universität Leipzig, Härtelstraße 16-18, 04107 Leipzig, Germany
5 LIFE – Leipzig Research Center for Civilization Diseases, Universität Leipzig, Härtelstraße 16-18, 04107 Leipzig, Germany
6 Fraunhofer Research Institution for Marine Biotechnology, Department of Medical Cell Technology, and Institute for Medical and Marine Biotechnology, University of Lübeck, Mönkhofer Weg 239a, 23562 Lübeck, Germany

Correspondence to: Michael A. Skeide,
Max Planck Institute for Human Cognitive and Brain Sciences,
Stephanstraße 1a, 04103 Leipzig,
Germany
E-mail: skeide@cbs.mpg.de

Keywords: dyslexia; visual word form area; NRSN1; imaging genetics; voxel-based morphometry

Abbreviations: SNP = single nucleotide polymorphism; VWFA = visual word form area

Received November 19, 2015. Revised April 13, 2016. Accepted May 8, 2016.

Introduction

The acquisition of reading and spelling skills requires thorough instruction and intensive training. As a consequence of this experience, an extended network of cortical areas is strongly reshaped. Functional specialization and structural transformation in the course of literacy acquisition have been demonstrated repeatedly for the left temporo-occipital cortex (Brem *et al.*, 2010; Dehaene *et al.*, 2010; Monzalvo *et al.*, 2012; Langer *et al.*, 2015), the left superior temporal cortex (Maurer *et al.*, 2007, 2009; Dehaene *et al.*, 2010; Monzalvo *et al.*, 2012; Linkersdorfer *et al.*, 2015), the left temporo-parietal cortex (Myers *et al.*, 2014; Linkersdorfer *et al.*, 2015), and the parieto-occipital cortex (Carreiras *et al.*, 2009). Unsurprisingly, the same regions are also affected in individuals suffering from developmental dyslexia (Paulesu *et al.*, 2001; Hoeft *et al.*, 2006, 2007; Blau *et al.*, 2010; Frye *et al.*, 2010; Lehongre *et al.*, 2011; Altarelli *et al.*, 2013; Finn *et al.*, 2014; Im *et al.*, 2016), a severe impairment of literacy acquisition considered as the most common learning disorder with a prevalence of 5 to 7% in the population (Peterson and Pennington, 2012; Moll *et al.*, 2014).

However, the variance in literacy achievement is not entirely explained by environmental factors. Instead, family studies have shown that there is also a heritable component (Hallgren, 1950; Bakwin, 1973; Gilger *et al.*, 1996; Harlaar *et al.*, 2005). By now, numerous single nucleotide polymorphisms (SNPs) on multiple genes and intergenic regions spanning several chromosomes have been found to be linked to literacy in association studies (see references provided in Supplementary Table 1). Moreover, there is MRI evidence that some of these SNPs are related to the haemodynamic functionality of dyslexia-relevant areas in left inferior frontal, superior temporal, and temporo-parietal cortices as well as their structural interconnections (Meda *et al.*, 2008; Cope *et al.*, 2012; Darki *et al.*, 2012; Pinel *et al.*, 2012; Wilcke *et al.*, 2012; Skeide *et al.*, 2015).

The goal of the present study was to identify potential relations between dyslexia candidate genes and brain macrostructure to investigate if such gene–brain association clusters can not only separate dyslexics from controls but also predict dyslexia before literacy onset. Dyslexia is defined here as significant difficulties in reading or spelling revealed by psychometric testing instead of by a formal diagnosis.

As a first step, we selected a set of 69 SNPs on 19 candidate genes that were previously reported to be linked with reading, spelling or other literacy-related language traits. To carry out a biologically valid analysis of the joint effects of SNPs located in the same gene, we set up a multi-locus model assessing gene-level associations with voxel-based morphometry measures in a sample of 141 children. Thereby, grey and white matter volume images were not reduced to predefined regions of interest to ensure an unbiased investigation of dyslexia risk gene effects on the whole brain. We were particularly interested in volumetric indices because of their suitability to capture potential dyslexia endophenotypes such as dendritic growth (Araki *et al.*, 2002), axonal growth (Araki *et al.*, 2002; Yue *et al.*, 2006), or dysregulated neuronal migration into cortical target layers (Galaburda and Kemper, 1979; Threlkeld *et al.*, 2007; Penagarikano *et al.*, 2011).

While it has been demonstrated that all genes analysed in this study are abundant as RNA in the brain (see the literature cited in Supplementary Table 1 and the developmental transcriptome database at http://www.brainspan.org/), the precise spatial distribution of their neural expression profiles is not yet fully explored. Accordingly, our hypothesis regarding the localization of the gene–brain association clusters was broad. We expected effects in multiple regions linked to literacy and dyslexia. For grey matter, these regions comprise the already mentioned left temporo-occipital cortex, the left superior temporal cortex, the left temporo-parietal cortex, the parieto-occipital cortex, and, additionally, the left inferior frontal cortex (Shaywitz *et al.*, 1998; Frye *et al.*, 2010; Boets *et al.*, 2013), the thalamus (Diaz *et al.*, 2012; Jednorog *et al.*, 2015), the cerebellum (Nicolson *et al.*, 1999), and the brainstem (Chandrasekaran *et al.*, 2009). For white matter, these regions comprise the local white matter next to the aforementioned grey matter areas (Klingberg *et al.*, 2000; Rimrodt *et al.*, 2010; Darki *et al.*, 2012) as well as the arcuate fasciculus (Vandermosten *et al.*, 2012; Yeatman *et al.*, 2012; Thiebaut de Schotten *et al.*, 2014) and the inferior fronto-occipital fasciculus (Vandermosten *et al.*, 2012).

As a second step, we used a linear binary support vector machine algorithm to classify children as dyslexic individuals and controls based on the genetically associated volumetric clusters. This subsample comprised two age groups. One group (the advanced literacy group) consisted of 34 participants that underwent MRI after at least 3 years of schooling between age 9 to 12 (grades 4 to 6) and were tested on average 1.7 years later, i.e. between age 10 to 14 (grades 4 to 8) for their reading and spelling skills to determine diagnostic status. The other group (the beginning literacy group) consisted of 20 participants, aged 5 to 6 years, from kindergartens not providing literacy instruction that underwent MRI at least 10 months before school entry to ensure that they had at best sporadic knowledge of letter-sound correspondences. The latter children were followed longitudinally to measure their reading and spelling performance at the end of the first grade. Individual measurement time points of the entire subsample are provided in Supplementary Table 2.

There is growing evidence that preliterate children at familial risk of dyslexia already show functional and structural alterations in temporo-parietal and temporo-occipital regions similar to those observed in diagnosed dyslexics (Raschle *et al.*, 2011, 2012; Hosseini *et al.*, 2013; Kraft *et al.*, 2015). Therefore, we predicted distinct morphometric signatures between dyslexic individuals and controls in the same cortical areas, not only in the literate brain at age 9 to 12 but also in the preliterate brain at age 5 to 6.

Table 1 Demographic information and psychometric performance of the cohort

	All	$Dys_{9\text{-}13}$[a]	Con_{Match}[b]	Δ[c]	$Dys_{5\text{-}6}$[d]	Con_{Match}[b]	Δ[c]
n	141	17	17	-	10	10	-
Age[e]	6.4 ± 2.7 (3.0–12.2)	10.4 ± 0.6 (9.4–11.4)	10.6 ± 0.8 (9.2–12.2)	$z = 0.55$ $P = 0.586$	5.6 ± 0.4 (5.1–6.3)	5.8 ± 0.2 (5.4–6.1)	$z = 1.217$ $P = 0.247$
Gender[f]	57/84	4/13	8/9	-	4/6	6/4	-
Handedness[g]	127/6/8	16/1/0	16/0/1	-	9/1/0	9/0/1	-
Parental education[h,i]	15 ± 4 (5–24)	13 ± 4 (6–23)	16 ± 5 (5–24)	$z = 2.23$ $P = 0.026^*$	13 ± 4 (7–20)	15 ± 3 (10–19)	$F = 1.167$ $P = 0.294$
Non-verbal IQ[h]	105 ± 14 (66–139)	114 ± 7 (100–126)	114 ± 9 (86–125)	$z = 0.59$ $P = 0.563$	110 ± 15 (90–137)	111 ± 13 (96–135)	$F = 0.002$ $P = 0.961$
Reading comprehension[h,j]	-[k]	23.0 ± 16.0 (9.0–56.0)	59.3 ± 17.2 (33.0–94.0)	$F = 25.753$ $P < 0.001^*$	10.4 ± 6.7 (2.1–21.5)	71.7 ± 24.0 (29.8–99.0)	$z = 3.585$ $P < 0.001^*$
Reading speed[h,j]	-[k]	21.0 ± 8.4 (8.0–32.0)	56.6 ± 20.2 (27.0–81.0)	$z = 3.671$ $P < 0.001^*$	31.4 ± 18.4 (0.5–50.5)	82.4 ± 17.6 (48.0–96.0)	$F = 36.074$ $P < 0.001^*$
Spelling accuracy[h,j]	-[k]	25.5 ± 27.4 (0.0–82.0)	65.9 ± 23.1 (32.0–99.0)	$z = 3.451$ $P < 0.001^*$	17.9 ± 13.7 (5.0–49.0)	57.0 ± 22.3 (31.0–88.0)	$z = 3.293$ $P < 0.001^*$

Dys = dyslexic; Con = control.

[a] Dyslexic individuals MRI scanned between age 9–12 and psychometrically diagnosed between 10–14 years of age.

[b] Controls matched according to MRI scan age.

[c] Statistic and *P*-value of the compared variable (asterisks indicate significant differences). *F* indices were derived from one-way ANOVAs (data normally distributed). *z* indices were derived from Mann-Whitney U-tests (data not normally distributed).

[d] Dyslexic individuals were MRI scanned at 5–6 years of age and psychometrically diagnosed at 7–8 years of age.

[e] MRI scan age in years, mean ± SD (minimum–maximum).

[f] Female/male.

[g] Right handers/left handers/ambidextrous [according to customized Edinburgh Handedness Inventory (Oldfield, 1971) laterality quotient (LQ)] [left-handedness defined as LQ < −28, i.e. the first decile value; right-handedness defined as LQ > 48, i.e. the first decile value; ambidexterity: −28 < LQ < +48)].

[h] Mean ± SD (minimum–maximum).

[i] Questionnaire-derived, single cumulative score per participating child computed by adding the sum of 2 scores (one per parent) for school education (4-point scale; no degree: 1 point; German 'Abitur': 4 points) and the sum of 2 scores (one per parent) for further education (9-point scale; no degree: 1 point; German 'Habilitation': 9 points).

[j] Literacy data are presented as standardized scores (percentile ranks).

[k] Literacy data of the entire cohort are not provided, because they were unavailable for 67 participants and because 20 additional participants could not be matched to the dyslexic individuals and were therefore not included in the MRI classification analyses which require equal sample sizes.

Materials and methods

Participants

One hundred and forty-one children were tested as part of the LEGASCREEN project (www.legascreen.de). Detailed demographic information of this cohort can be found in Table 1. Participants were recruited mainly from the Leipzig metropolitan area but also from other parts of Germany through our homepage, newspaper announcements, magazine articles, a television documentary and talks in local schools and speech therapy centres. Families with a history of developmental dyslexia were particularly encouraged to participate. All parents completed a questionnaire revealing that no participant had a history of neurologically or psychiatrically relevant diseases. All children that met these two selection criteria, and of whom high-quality MRI scans could be taken, were included in the present study. All parents gave written informed consent while their children gave documented verbal assent to participate in the study. All experimental procedures were approved by the University of Leipzig Ethical Review Board.

Psychometric data acquisition

Non-verbal IQ

IQ scores of all children MRI-scanned at age 6 or below were determined using the performance subscale of the Wechsler Preschool and Primary Scale of Intelligence (WPPSI-III) (Wechsler, 2009). IQ scores of all children MRI-scanned at age 9 or above were determined using the Kaufman Assessment Battery for Children (K-ABC) (Kaufman et al., 2003). For additional details, see Supplementary material.

Reading comprehension and reading speed

In children between grade 1 and 6, reading comprehension was tested with the 'Ein Leseverständnistest für Erst- bis Sechstklässler' (ELFE 1-6; translation: Reading comprehension test for grades 1 to 6) (Lenhard and Schneider, 2006) and reading speed was tested with the 'Weiterentwicklung des Salzburger Lese- und Rechtschreibtests' (SLRT-II; translation: Improved Salzburg reading and orthographic writing test) (Moll and Landerl, 2010). In children attending grade 7 or 8, both reading comprehension and reading speed were tested with the 'Lesegeschwindigkeits- und -verständnistest für die Klassen 6-12' (LGVT; translation: Reading speed and reading comprehension test for grades 6 to 12) (Schneider *et al.*, 2007).

Spelling accuracy

Performance in spelling (writing after dictation) was assessed with the grade-appropriate versions of the 'Deutscher Rechtschreibtest' (DERET; translation: German spelling test) (Stock and Schneider, 2008*a*, *b*).

Criterion for the diagnosis of developmental dyslexia

Following current German guidelines, we applied dual diagnostic criteria of developmental dyslexia. Individuals were categorized as being dyslexic if they scored equal to or below the 15th percentile rank of the population performance either in the reading comprehension, the reading speed, or the spelling accuracy test, given that their IQ was not more than 1 standard deviation (SD) below the population average (≥ 85). In addition, individuals were also categorized as being dyslexic if their score lay within the 25th percentile rank in one of the mentioned tests and was at least 1 SD below the level expected based on the child's IQ according to a regression criterion (Schulte-Korne, 2010). Our approach was more liberal than the clinical practice guideline as participants had to perform below threshold only in one but not in all of the tests in order to meet the diagnostic criterion. However, we consider this an appropriate compromise as our approach is still more conservative than a frequently used criterion requiring sub-25th percentile performance in a single subtest (Tanaka *et al.*, 2011; Finn *et al.*, 2014).

The inclusion of spelling as a sufficient criterion in the diagnosis of dyslexia might have inflated the proportion of cases in the beginning literacy group. However, in this subsample there was only 1 of 10 dyslexic individuals that only had spelling accuracy deficits but neither reading comprehension nor reading speed deficits. Accordingly, the risk of having identified a false-positive case seems to be limited to a single participant. Nine of ten dyslexic individuals in the beginning literacy group showed reading comprehension deficits, which seems to be the primary sign of dyslexia after the first year of school instruction. It remains open, if spelling accuracy deficits alone represent a reliable diagnostic criterion of dyslexia in German first graders.

Literacy achievement data were only available for 74 of 141 participants. First, 27 participants (17 individuals of the advanced literacy group and 10 individuals of the beginning literacy group) were identified as dyslexics. An equal number of 27 control participants scoring above threshold was selected from the remaining sample of 47 participants for which literacy data were available (advanced literacy group: 20 participants; beginning literacy group: 27 participants) to best match the cases in terms of age, gender, handedness, IQ, and parent education. Group differences according to these variables yielded a significance threshold of $P > 0.2$ with the exception of parental education in the older group (Table 1).

Genotyping

Genotypic information was collected for 69 SNPs documented in the literature as significantly associated with reading, spelling, phonological processing, articulation, and vocabulary (Supplementary Table 1). DNA was extracted from saliva applying standard procedures (Quinque *et al.*, 2006) or using Oragene DNA Genotek Kits (Kanata). Two different techniques were used. Initially, 59 SNPs were genotyped with the matrix-assisted laser desorption/ionization time-of-flight mass spectrometry system iPLEX® (Agena). This set was complemented with eight SNPs from the bead chip Infinium HumanCoreExome Psych Chip. The bead chip genotyping was performed according to the manufacturer's protocols and data were processed using the GenomeStudio Genotyping Module (Illumina). Two SNPs not covered by the iPLEX® technique or by the bead chip were replaced with proxy SNPs revealing the largest linkage to the original candidate (Supplementary Table 1). Only SNPs with a minor allele frequency (MAF) >0.10 and a call-rate $>97\%$ were included for analysis. SNPs were not allowed to violate Hardy-Weinberg-Equilibrium (HWE) ($P > 0.05$, family-wise error corrected) and each genotype had to be present in at least five individuals. Individuals with a call-rate $<95\%$ were excluded and non-relatedness among all individuals was ensured by principal component analyses of the kinship (identity by state) measures between the participants. The maximum accepted identity by state was set to 0.125. All quality control parameters were estimated using GenABEL (Aulchenko *et al.*, 2007) and R (http://www.r-project.org/). The final set of 69 SNPs on 19 genes covering eight chromosomes together with the corresponding numbers of participants in each genotypic category and the MAF are listed in Supplementary Table 1.

Voxel-based morphometry analysis

The T_1 images acquired in the present study (see Supplementary material for details) passed a two-stage quality assessment procedure. As a first step, each image was visually inspected for coarse artefacts. As a second step, the exact covariance between all volume images was calculated to include only those images with a covariance coefficient within 2 SD of the mean.

For the voxel-based morphometry analysis, we used version 8 of the Voxel-based Morphometry Toolbox (http://dbm.neuro.uni-jena.de/vbm.html) implemented in the Statistical Parametric Mapping 8 software (http://fil.ion.ucl.ac.uk/spm/). First, the images were normalized to an age-specific template in Montreal Neurological Institute (MNI) space that was directly derived from the sample by employing the Diffeomorphic Anatomical Registration Through Exponentiated Lie Algebra (DARTEL) algorithm (Ashburner, 2007). Second, the images were segmented into grey matter, white matter, CSF, dura, non-brain soft tissue and air. Tissue probability maps used as priors for the segmentation were customized using the Template-O-Matic Toolbox Version 8 (https://irc.cchmc.org/software/tom/downloads.php) to reflect age and gender of the present sample. As the toolbox only provides reference data in the age range of 5–18 years, all 38 children from our sample that are below this age were treated as 5-year-old children. Tissue probability maps of 5-year-old children are considered as sufficiently reliable priors for the segmentation of 3-year-olds' brain images. Despite the proven superior brain tissue differentiation of MP2RAGE scans compared to conventional MPRAGE scans (Marques *et al.*, 2010), we applied a tissue probability threshold of 0.15, which is slightly more conservative than the commonly used threshold of 0.1. The rationale behind this choice was to minimize the risk of voxel misclassification at tissue boundaries while at the same time keeping as many voxels as possible in the analysis. Grey matter and white matter maps were modulated for non-linear effects to preserve local volumetric values while accounting for individual differences in total intracranial volume. Finally, the images were smoothed with an 8 mm full-width at half-maximum Gaussian kernel.

Cluster-wise gene association analysis

Relations between genes and volume images were explored as previously described (Ge *et al.*, 2012). In short, the approach

combines cluster-wise statistical inference within brain images based on the random field theory with a multivariate non-parametric genetic model based on least-squares kernel machines. *P*-values are estimated accurately with a time-efficient permutation procedure based on parametric tail approximation. The method ensures statistical validity as it models the nonlinearity of SNP effects with high sensitivity and as it is robust to missing SNP data. A multi-locus model was set up for each brain tissue class to test for the joint effect of SNPs in a gene. Age, gender, handedness and parental education were included as covariates of no interest in the model.

Clusters were defined as connected voxels sharing at least a corner (i.e. 26 voxels) and assessed for significance by applying a 3-step multiple comparison correction procedure: First, a type I error threshold was set to $P < 0.001$. Moreover, the sizes of the remaining clusters were adjusted according to the local smoothness of the data to avoid potential type I and type II errors caused by non-stationarity, i.e. non-isotropic smoothness, of the volumetric images (Worsley *et al.*, 1999). Second, spatial extent thresholds at $P < 0.001$ were obtained running 10 000 iterations of a Monte Carlo Simulation as implemented in the AlphaSim tool (http://afni.nimh.nih.gov/). This procedure revealed minimum cluster size cut-offs of $k = 322$ voxels (for 449 972 grey matter voxels) and $k = 249$ (for 212 870 white matter voxels). Finally, a family-wise error correction for the 19 tested genes was performed. We favoured a cluster-based over a voxel-wise approach because the latter is agnostic to any spatial correlation between voxels and thus might decrease power to detect regions that show valid effects. Images were visualized using the Mango toolbox (http://ric.uthscsa.edu/mango/). The anatomical labels, sizes, MNI coordinates and maximum *P*-values of all surviving clusters can be found in Supplementary Tables 3 and 4.

Multivariate pattern classification analysis

The Pattern Recognition for Neuroimaging Toolbox (http://www.mlnl.cs.ucl.ac.uk/pronto) was used to classify a subsample of 54 children (34 participants that underwent MRI between 9 to 12 years of age and 20 participants that underwent MRI between 5 to 6 years of age) into dyslexic individuals and controls using the nine volume clusters that showed a significant association with a gene. Nine separate classifiers were trained with a linear binary support vector machine, one on each of the nine regions of interest (i.e. the images containing all in-mask volume-labelled voxels for each participant). We applied a 10-fold cross-validation, so that each classifier was first trained on a random subset of 90% of the images and then tested for its performance on the remaining 10% of the images. All images were mean-centred during cross-validation.

Post hoc, we tested to which degree the individual volumetric profile within a region of interest is related to the individual level of parental education. For this purpose, a kernel ridge regression analysis was carried out on a random subset of 90% of the mean-centred region of interest images before assessing the accuracy on the remaining 10%. The same approach was applied to the grey matter volume images when testing for the region of interest- and whole-brain level correlates of literacy skills, i.e. percentile ranks of reading comprehension, reading speed, and spelling accuracy.

For all statistical models, *P*-values were determined non-parametrically via permutation tests iteratively running 10 000 permutations. The *P*-values obtained from the classification were family-wise error corrected for all region of interest-wise tests within each modality (separately for grey matter and white matter volume). The *P*-values obtained from the regression analyses were family-wise error corrected for the three types of literacy skills tested.

Tests of associations between dyslexia candidate genes and literacy skills

To investigate the joint effects of all SNPs of each individual gene on the individual dyslexia diagnosis and on literacy skills, respectively, we constructed two models (separately for each gene). The first model only included the intercept and the covariates parental education and age. The second model included the same covariates and, in addition, all SNPs of each gene of interest. Finally, both models were compared using a likelihood ratio test to capture the additional effects of the SNPs using the package 'testing linear regression models' implemented in the R software (https://cran.r-project.org/web/packages/lmtest/). All *P*-values derived from these analyses were family-wise error corrected for the number of genes tested.

Results

Dyslexia candidate gene associations with grey and white matter volume

Significant associations with grey matter volume at a threshold of $P < 0.001$ (corrected) were found for 3 of 19 genes, namely *NRSN1*, *FOXP2*, and *COL4A2*. Effects of *NRSN1* were distributed over three clusters located in the right dorsal parieto-occipital cortex (MNI coordinates: 42, −18, 53 / 35, −71, 41 / 29, −48, 57), the left lateral occipital cortex (−9, −83, 42) and the left temporo-occipital fusiform cortex (−33, −63, −18), also known as the 'visual word form area' (VWFA). *FOXP2* showed an association in the left medial superior frontal gyrus (−3, 38, 53). *COL4A2* was found to be related to a cluster in the right cerebellum (17, −77, −54) (Fig. 1A, B, and Supplementary Fig. 1).

NRSN1, *CNTNAP2* and *CMIP*, i.e. 3 of the 19 genes, revealed significant associations with white matter volume ($P < 0.001$, corrected). *NRSN1* was related to a cluster in the local white matter of the left postcentral cortex (−45, −23, 60), *CNTNAP2* was related to the left cerebral and cerebellar peduncles (−20, −27, −8 / −11, −41, −45), and *CMIP* was related to bilateral portions of cerebellar white matter (−9, −83, 42 / 32, −68, −36) (Fig. 1C, D and Supplementary Fig. 2).

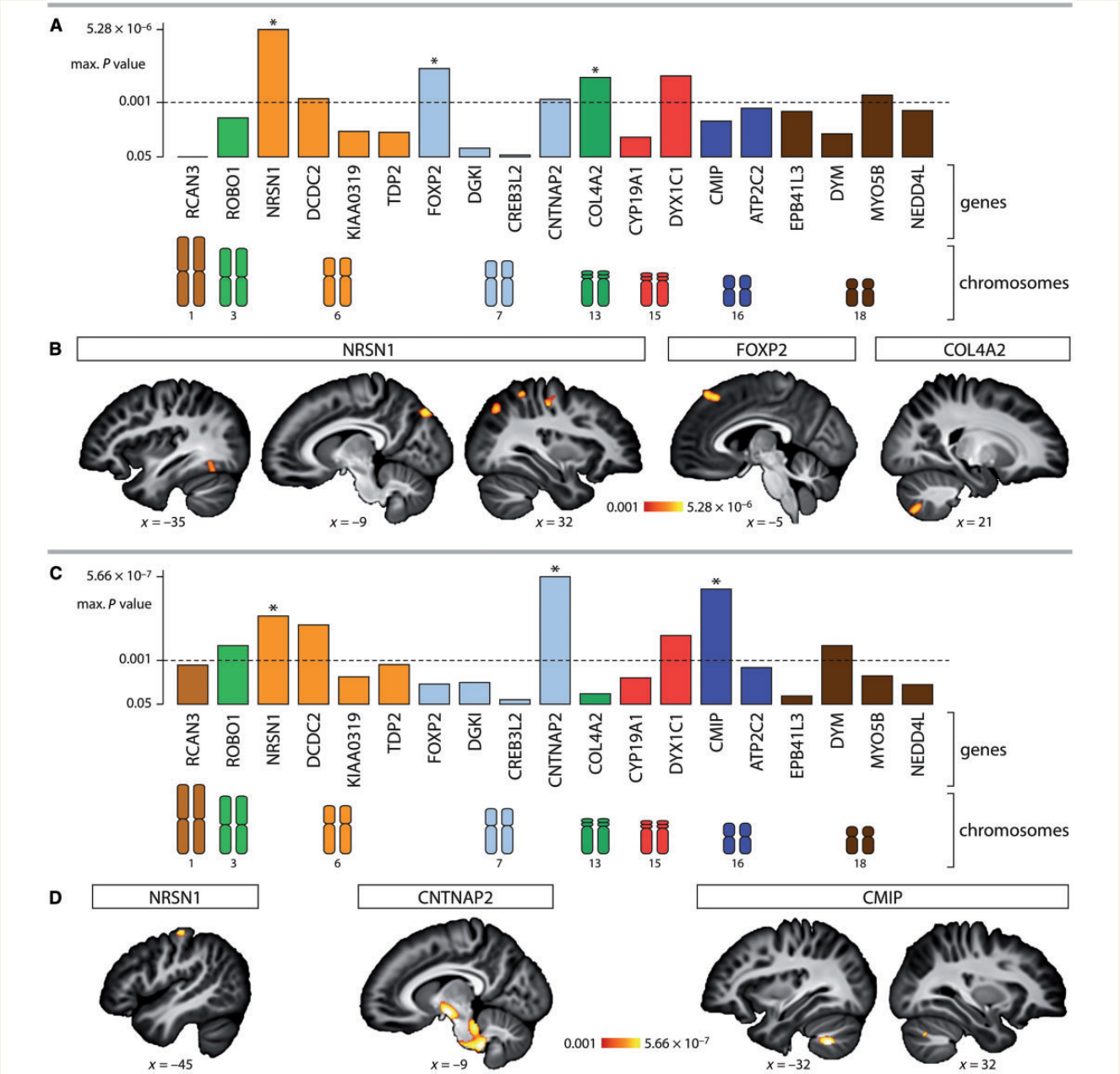

Figure 1 Associations of dyslexia candidate genes with grey and white matter volume. The *x*-axes of the diagrams depict 19 candidate genes colour-coded for the eight chromosomes they belong to. These genes are known from the literature to be significantly associated with reading, spelling or other language-related behavioural traits. The *y*-axis in **A** represents the maximum *P*-values of the associations between the genes and the grey matter volume images. The *y*-axis in **C** represents the maximum *P*-values of the associations between the genes and the white matter volume images. The dashed line represents the corrected threshold of $P = 0.001$. Asterisks indicate genetically associated clusters that remain significant after correction for type I error, spatial extent and number of genes tested. Note that bars crossing the dashed line without receiving an asterisk only passed the type I error but not the spatial extent correction and thus were not considered significant. (**B**) *P*-value images showing all grey matter volume clusters that revealed a significant association with the genetic variants *NRSN1*, *FOXP2* and *COL4A2*. (**D**) *P*-value images showing all white matter volume clusters that revealed a significant association with the genetic variants *NRSN1*, *CNTNAP2* and *CMIP*. The letter 'x' indicates the MNI coordinate of the sagittal cut plane. The colour bars indicate the range of the *P*-values. All presented *P*-values are corrected for multiple testing. The exact *P*-values of the most significant voxels within the clusters as well as the *P*-value images from transversal and coronal perspectives can be found in Supplementary Figs 1 and 2.

The models were adjusted for the effects of age and total intracranial volume to capture specific genetic associations with volumetric profiles independent of general maturational trajectories. Furthermore, the effect of parental education was also removed from the data to focus on gene–brain associations that are not mediated by factors reflecting literacy-related experiences in the early home environment. Cluster sizes and exact *P*-values are listed in Supplementary Tables 3 and 4.

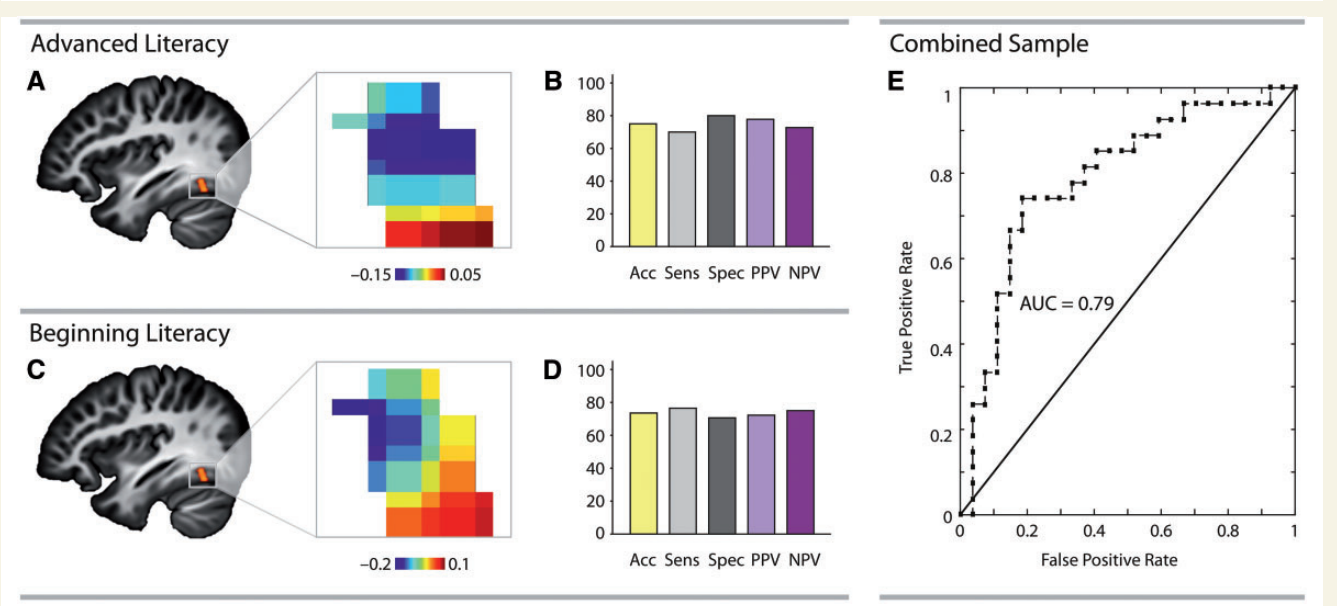

Figure 2 Classification of dyslexics and controls with the genetically associated grey matter volume profile of the visual word form area. Binary support vector machine classification weight maps are presented separately for two subsamples. (**A**) Thirty-four children in a stage of advanced literacy, MRI-scanned and psychometrically diagnosed for dyslexia in grades 4 to 7 (17 dyslexics versus 17 controls). (**C**) Twenty children in a beginning stage of literacy, MRI-scanned at a kindergarten age before literacy instruction and psychometrically diagnosed for dyslexia at the end of first grade (10 dyslexics versus 10 controls). The colour bars indicate the range of classification weights. Five classification indices are displayed separately on the *x*-axis for **B** the advanced literacy group, and for **D** the beginning literacy group (Acc = total classification accuracy; Sens = sensitivity; Spec = specificity; PPV = positive predictive value; NPV = negative predictive value). The *y*-axis displays the classification performance (0 to 100%). All classification indices for all regions of interest including the remaining eight grey and white matter volume clusters are provided in Supplementary Figs 3 and 4. (**E**) Receiver operating characteristic curve illustrating the performance of the classifier in the combined sample of 27 dyslexic participants and 27 controls. The *y*-axis represents the true positive rate, i.e. the rate of individuals that were correctly identified as cases, and the *x*-axis represents the false positive rate, i.e. the rate of individuals that were correctly identified as controls. The overall performance of the classifier is quantified as the area under the receiver operating characteristic curve (AUC).

Classification of dyslexics and controls with the genetically associated volume profiles

Initially, case-control classification performance was tested separately for each of the significant clusters derived from the association analysis in the sample of 9- to 12-year-old children. Of the five grey matter and four white matter volume clusters, only the grey matter volume cluster located in the VWFA performed significantly above chance classifying the participants into dyslexic and control individuals (total classification accuracy: 73.53%, $P = 0.031$, corrected) (Fig. 2A and B). Subsequently, this analysis was also carried out in the sample of 5- to 6-year-old children to evaluate if their structural brain data at a preliterate age had the distinctive power to identify young dyslexics and controls after one school year of literacy instruction. Again, the classification performance of the grey matter volume cluster located in the VWFA reached significance (total classification accuracy: 75%, $P = 0.035$, corrected) (Fig. 2C and D) in addition to the grey matter volume cluster located in the left lateral parieto-occipital cortex (total classification accuracy: 80%, $P = 0.028$, corrected). The detailed classification performance of all clusters can be found in Supplementary Figs 3 and 4. In the combined sample, the classifier trained on the VWFA region of interest distinguished cases from controls with a true positive rate of 0.74 and a false positive rate of 0.81, revealing an area under the receiver operator characteristic curve of 0.79 (Fig. 2E). Moreover, a kernel ridge regression within the region of interest revealed a significant association with reading comprehension ($R^2 = 0.07$, $P = 0.025$, corrected) and reading speed ($R^2 = 0.06$, $P = 0.047$, corrected), but not with spelling accuracy ($R^2 = 0.01$, $P = 0.480$, corrected).

Finally, as it was not possible to match dyslexics and controls in the advanced literacy group with respect to parental education, we evaluated to which degree this variable was related to the volumetric profile of the VWFA. However, a kernel ridge regression within the VWFA failed to detect any volumetric spatial pattern that explained variance in parental education, both in the advanced literacy group ($R^2 = 0.00$, $P = 0.904$) and in the beginning literacy group ($R^2 = 0.00$, $P = 0.981$).

Whole-brain grey matter volume correlates of individual literacy skills

We also aimed to identify brain areas related to individual variation in literacy skills independent of the genetic

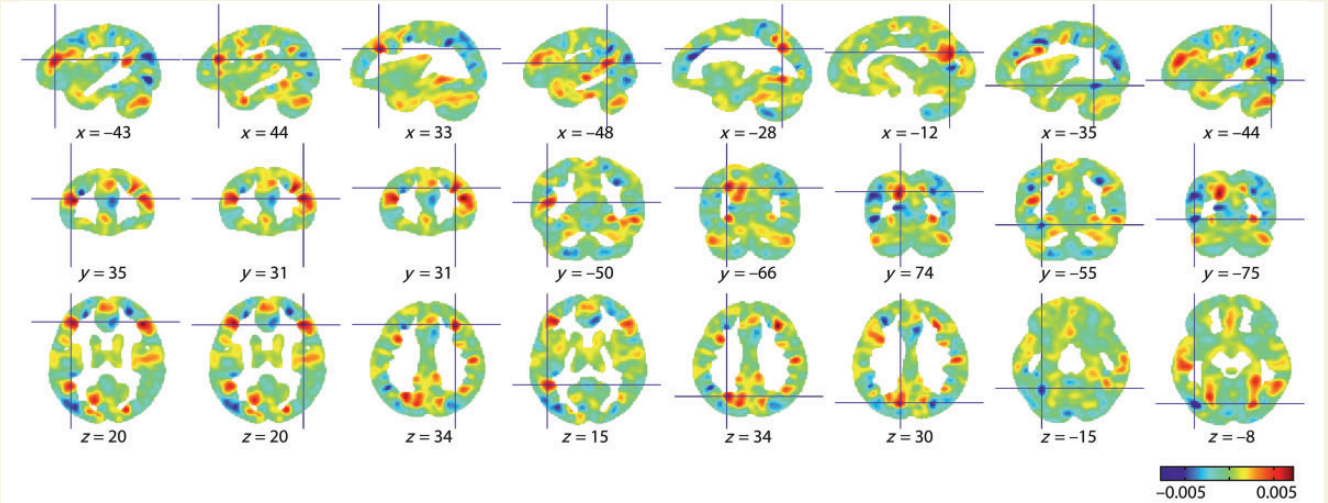

Figure 3 Whole-brain grey matter volume correlates of individual reading speed. Depicted are kernel ridge regression weight maps with cross-hairs over regions where weights exceeded the threshold of −0.005 (blue) or 0.005 (red). The colour bar indicates the range of the regression weights. The letters *x*, *y* and *z* specify the MNI coordinates of the sagittal, coronal and transversal cut planes, respectively. Non-significant grey matter volume associations with individual reading comprehension performance and with individual spelling accuracy are provided in Supplementary Fig. 5.

variants tested. Therefore, we ran whole-brain-level kernel ridge regression analyses to determine to which degree each voxel in each grey matter volume image is related to each of the 54 participants' performance in the reading comprehension, reading speed, and spelling accuracy tests, respectively. A significant association was found for reading speed ($R^2 = 0.15$, $P = 0.035$, corrected). Voxels with the highest positive relative weight were located in the bilateral middle frontal gyri (−43, 35, 20 / 44, 31, 20 / 33, 31, 34), the left posterior superior temporal gyrus (−48, −50, 15), and the left parieto-occipital cortex (−28, −66, 34 / −12, 74, 30). Clusters in the VWFA (−35, −55, −15) and the left visual cortex (−44, −75, −8) revealed the highest negative weights (Fig. 3). No significant whole-brain-level associations were found for reading comprehension ($R^2 = 0.03$, $P = 0.2916$, corrected) and spelling accuracy ($R^2 = 0.05$, $P = 0.2715$, corrected) (Supplementary Fig. 5).

Associations between dyslexia candidate genes and individual literacy skills

To further support the current evidence from the literature that the SNPs rs9356928, rs4285310 and rs3178 on *NRSN1* are related to dyslexia, we computed their joint association with the individual diagnostic status (dyslexic versus control) of each participant. This effect reached statistical significance [$\chi(3) = 8.18$, $P = 0.042$].

We also observed significant associations between the individual reading comprehension performance and the genes *NRSN1* [$\chi(3) = 14.54$, $P = 0.002$], *KIAA0319* [$\chi(3) = 7.86$, $P = 0.049$], *CNTNAP2* [$\chi(6) = 13.77$, $P = 0.032$], and *CMIP* [$\chi(5) = 18.69$, $P = 0.002$]. Moreover, individual reading speed was significantly associated with *KIAA0319* [$\chi(3) = 9.77$, $P = 0.021$] and *TDP2* [$\chi(1) = 4.378$, $P = 0.036$]. The association between *NRSN1* and reading comprehension turned out to remain significant when family-wise error correcting for the number of all tested genes. Full results of all association tests are provided in Supplementary Table 5.

Discussion

Here, we investigated associations between 19 candidate genes reported to be linked to literacy skills and the relative volume of the grey and the white matter in a cohort of 141 children ranging from age 3 to 12. The genes *NRSN1*, *FOXP2*, and *COL4A2* turned out to be significantly related to grey matter regions known to support functions that play a role for literacy. The genes *NRSN1*, *CNTNAP2*, and *CMIP* were found to be significantly related to white matter regions known to be part of the structural network underlying literacy proficiency. Within a grey matter cluster in the VWFA that was significantly associated with *NRSN1*, we detected volumetric patterns that classified dyslexic individuals, defined as not being formally diagnosed, but as showing substantial difficulties in psychometric tests of reading or spelling, and control individuals with significant above-chance performance. These patterns were found in a sample of 17 dyslexics and 17 control subjects MRI-scanned at age 9 to 12 (grades 4 to 6) and assessed for literacy skills on average 1.7 years later at age 10 to 14 (grades 4 to 8), and, moreover, in a sample of 10 dyslexics and 10 control subjects MRI-scanned at age 5 to 6 (attending kindergarten) and assessed for literacy skills

at age 7 to 8 (end of the first grade). In the latter sample, an additional significantly classifying volumetric pattern was found in the left lateral occipital cortex that was also associated with *NRSN1*. All effects were statistically independent of the participants' age, gender and handedness, as well as the educational level of their parents. The grey matter volume of the VWFA was significantly associated with reading comprehension and reading speed, but not with spelling accuracy. A significant association with reading speed, but neither with reading comprehension nor with spelling accuracy, was also found at the whole-brain level in several grey matter regions known to support reading acquisition. In line with previous evidence from the literature (Deffenbacher *et al.*, 2004; Couto *et al.*, 2010), *NRSN1* was significantly related to the individual dyslexia diagnosis and the individual reading comprehension skills. Further significant associations with reading comprehension were observed for the genes *KIAA0319*, *CNTNAP2* and *CMIP*. Reading speed was significantly related to *KIAA0319* and *TDP2*.

Our observation that *NRSN1* was related to both grey and white matter volume is corroborated by *in vitro* evidence indicating that the protein encoded by this gene is involved in neurite extension by transporting vesicles to the growing ends of dendrites and axons (Araki *et al.*, 2002). A similar role during early brain development is also ascribed to *FOXP2* (Vernes *et al.*, 2011), which revealed an association with grey matter volume in the present study. The neuromolecular mechanisms regulated by *COL4A2* and its potential link to the grey matter, however, are currently unclear and require further investigation (Verbeek *et al.*, 2012). Supporting previous studies, the relation between *CNTNAP2* and white matter volume revealed by our study is in line with the finding that its protein product contributes to the clustering of potassium channels at juxtaparanodes of axons which is vital for intact neuronal signalling (Rodenas-Cuadrado *et al.*, 2014). Finally, *CMIP* was also associated with white matter volume, but its microstructural functions in the maturing brain are not yet uncovered (Wang *et al.*, 2015).

The neurobiological validity of the genetic association clusters with respect to the transcriptome of the dyslexic brain might be best evaluated on the basis of future post-mortem work shedding light on the neural expression landscape of the dyslexia candidate genes. Nevertheless, all effects were localized in brain areas that have been linked to literacy or dyslexia in previous studies. The VWFA is part of the ventral visual stream that becomes increasingly sensitive to print when reading and spelling is learnt (Dehaene *et al.*, 2015). A dorsal functional network including parieto-occipital and superior frontal cortices is assumed to influence how well readers can allocate top-down attentional resources to the visual discrimination of letters (Finn *et al.*, 2014). The cerebellum and also pre- and postcentral cortices are thought to support the automatization of both explicitly and implicitly learned skills, which is crucial for fluent reading and spelling (Nicolson *et al.*, 1999; Menghini *et al.*, 2006, 2008). There is evidence that the auditory brainstem plays a role for encoding basic acoustic features of speech sounds and thus affects the quality of phonological representations (Chandrasekaran *et al.*, 2009). The left cerebellar peduncle could be a pathway over which basic acoustic information is propagated from the brainstem to the thalamus for further acoustic processing. This hypothesis should be tested in follow-up studies. Finally, the relation of the left cerebral peduncle to *CNTNAP2* and its possible contribution to literacy also remains to be further assessed.

It has been argued that it is almost impossible to isolate structural brain changes underlying childhood literacy acquisition owing to unspecific maturational changes and uncontrollable environmental differences (Carreiras *et al.*, 2009). Indeed, existing data on volumetric differences between dyslexic and control individuals have been ambiguous so far. On the one hand, there are studies suggesting that higher grey matter volume in temporo-parietal and temporo-occipital regions relate to higher literacy skills (Silani *et al.*, 2005; Hoeft *et al.*, 2007). On the other hand, there are studies suggesting that lower grey matter volume in temporo-parietal regions relate to higher literacy skills (Darki *et al.*, 2012, 2014). Here we resolved this ambiguity by sidestepping this dichotomy and accommodating the possibility that cortical disparities between dyslexics and controls might be averaged out when simply testing for mean differences between them. Instead, we argue that the disparities follow rather complex spatial distributions that are more adequately represented by volumetric patterns. The specificity of our results is additionally bolstered by the fact that we removed the effects of total intracranial volume and age in our models to account for interindividual and age-related differences in maturation, particularly synaptic pruning.

Our knowledge about the role of the environment in literacy acquisition is still limited. Nevertheless, there is evidence that genetic contributions to dyslexia increase while environmental contributions decrease the higher the level of parental education (Friend *et al.*, 2008). It is assumed that the educational level of parents is related to the language and literacy skills of their children. These skills are in turn considered protective factors of dyslexia for children in the home literacy environment (Lyytinen *et al.*, 2004; Peterson and Pennington, 2012; van der Leij *et al.*, 2013). Importantly, we ruled out the plausible possibility that the effect of *NRSN1* on the VWFA could be explained by parental education as we controlled for this factor in our models. Furthermore, there was no indication that the case–control classification performance of the VWFA could have been blurred by latent variables related to parental education. It is certain that the present study does not allow us to estimate how much variance in literacy phenotypes can be explained by genetic relations to the VWFA compared to environmental influences on the VWFA. Nevertheless, it allows us to reason that the association of *NRSN1* with the VWFA specifically explains a certain portion of variance in dyslexia independently of parental education, the variable that best reflects the most proximate

environmental mediator currently known. An exact quantification of the unique and shared contributions of genetic and environmental factors to the literate brain remains as a major future challenge for the field.

We acknowledge that the regions affected in dyslexic individuals might also vary as a function of their cognitive deficits (Heim and Grande, 2012) and of their age. The latter aspect is supported by our observation that a pattern in the left lateral parieto-occipital cortex significantly separated dyslexics from controls before literacy instruction but not after at least 3 years of schooling. At the same time, we emphasize that our results provide evidence for an endophenotypic continuum of *NRSN1* polymorphisms in relation to volumetric features of the VWFA. Further experiments are needed to corroborate the view that fluctuating and stable endophenotypes co-occur in developmental dyslexia.

Limitations

It should be noted that our sample of 141 participants is considered small for a genetic association analysis. Moreover, the current study does not include an external replication sample. The feasibility of larger follow-up analyses depends on the possibility to combine the data of our cohort with data from other cohorts from populations that are comparable in terms of orthographic transparency and genetic homogeneity. Furthermore, it should be acknowledged that the original *NRSN1*-related SNP rs4285310 was not covered by the genotyping techniques used and therefore replaced by the proxy SNP rs10946673 in the present analyses (Supplementary Table 1).

To provide a reliable literacy assessment after only 1 year of schooling, we made sure that all participants were familiar with the core German alphabet and fully understood all tasks (Supplementary material). Moreover, the reliability of the diagnostic categorization is bolstered by the fact that the classification of dyslexics and controls with the genetically associated volume profiles revealed a comparable performance in the first-graders compared to an independent sample of children with more advanced literacy skills. Nevertheless, we acknowledge that there are potential other sources that might decrease the reliability of diagnosing dyslexia after the first school year.

Conclusion

The present study sheds new light on the interplay of 'nature and nurture' during literacy acquisition. Justifiably, the VWFA is a prime example of how learning-induced cortical plasticity leads to an expansion of the human cognitive repertoire. Here, we have shown, however, that there seems to be a genetic limit to the adaptivity of this region to literacy-related skills. The grey matter volume of the VWFA was found to be related to *NRSN1*, a gene assumed to regulate neurite growth from early maturation stages on. Moreover, the *NRSN1*-associated cluster in the VWFA robustly distinguished dyslexics and controls not only after several years of schooling, but also already at a kindergarten age before literacy instruction had actually begun. There was no indication that these effects could have been mediated by environmental influences reflecting parental education levels. Nevertheless, the genetic and environmental dynamics underlying the pivotal role of the VWFA for literacy acquisition require further investigation in large-scale future studies.

Funding

This work was funded by the Max Planck Society and the Fraunhofer Society (Grant number: M.FE.A.NEPF0001).

Supplementary material

Supplementary material is available at *Brain* online.

References

Altarelli I, Monzalvo K, Iannuzzi S, Fluss J, Billard C, Ramus F, et al. A functionally guided approach to the morphometry of occipitotemporal regions in developmental dyslexia: evidence for differential effects in boys and girls. J Neurosci 2013; 33: 11296–301.

Araki M, Nagata K, Satoh Y, Kadota Y, Hisha H, Adachi Y, et al. Developmentally regulated expression of Neuro-p24 and its possible function in neurite extension. Neurosci Res 2002; 44: 379–89.

Ashburner J. A fast diffeomorphic image registration algorithm. Neuroimage 2007; 38: 95–113.

Aulchenko YS, Ripke S, Isaacs A, Van Duijn CM. GenABEL: an R library for genome-wide association analysis. Bioinformatics 2007; 23: 1294–6.

Bakwin H. Reading disability in twins. Dev Med Child Neurol 1973; 15: 184–7.

Blau V, Reithler J, van Atteveldt N, Seitz J, Gerretsen P, Goebel R, et al. Deviant processing of letters and speech sounds as proximate cause of reading failure: a functional magnetic resonance imaging study of dyslexic children. Brain 2010; 133 (Pt 3): 868–79.

Boets B, Op de Beeck HP, Vandermosten M, Scott SK, Gillebert CR, Mantini D, et al. Intact but less accessible phonetic representations in adults with dyslexia. Science 2013; 342: 1251–4.

Brem S, Bach S, Kucian K, Guttorm TK, Martin E, Lyytinen H, et al. Brain sensitivity to print emerges when children learn letter-speech sound correspondences. Proc Natl Acad Sci USA 2010; 107: 7939–44.

Carreiras M, Seghier ML, Baquero S, Estevez A, Lozano A, Devlin JT, et al. An anatomical signature for literacy. Nature 2009; 461: 983–6.

Chandrasekaran B, Hornickel J, Skoe E, Nicol T, Kraus N. Context-dependent encoding in the human auditory brainstem relates to hearing speech in noise: implications for developmental dyslexia. Neuron 2009; 64: 311–19.

Cope N, Eicher JD, Meng H, Gibson CJ, Hager K, Lacadie C, et al. Variants in the DYX2 locus are associated with altered brain activation in reading-related brain regions in subjects with reading disability. Neuroimage 2012; 63: 148–56.

Couto JM, Livne-Bar I, Huang K, Xu Z, Cate-Carter T, Feng Y, et al. Association of reading disabilities with regions marked by acetylated

H3 histones in KIAA0319. Am J Med Genet B Neuropsychiatr Genet 2010; 153B: 447–62.
Darki F, Peyrard-Janvid M, Matsson H, Kere J, Klingberg T. Three dyslexia susceptibility genes, DYX1C1, DCDC2, and KIAA0319, affect temporo-parietal white matter structure. Biol Psychiatry 2012; 72: 671–6.
Darki F, Peyrard-Janvid M, Matsson H, Kere J, Klingberg T. DCDC2 polymorphism is associated with left temporoparietal gray and white matter structures during development. J Neurosci 2014; 34: 14455–62.
Deffenbacher KE, Kenyon JB, Hoover DM, Olson RK, Pennington BF, DeFries JC, et al. Refinement of the 6p21.3 quantitative trait locus influencing dyslexia: linkage and association analyses. Hum Genet 2004; 115: 128–38.
Dehaene S, Cohen L, Morais J, Kolinsky R. Illiterate to literate: behavioural and cerebral changes induced by reading acquisition. Nat Rev Neurosci 2015; 16: 234–44.
Dehaene S, Pegado F, Braga LW, Ventura P, Nunes G, Jobert A, et al. How learning to read changes the cortical networks for vision and language. Science 2010; 330: 1359–64.
Diaz B, Hintz F, Kiebel SJ, von Kriegstein K. Dysfunction of the auditory thalamus in developmental dyslexia. Proc Natl Acad Sci USA 2012; 109: 13841–6.
Finn ES, Shen X, Holahan JM, Scheinost D, Lacadie C, Papademetris X, et al. Disruption of functional networks in dyslexia: a whole-brain, data-driven analysis of connectivity. Biol Psychiatry 2014; 76: 397–404.
Friend A, DeFries JC, Olson RK. Parental education moderates genetic influences on reading disability. Psychol Sci 2008; 19: 1124–30.
Frye RE, Liederman J, Malmberg B, McLean J, Strickland D, Beauchamp MS. Surface area accounts for the relation of gray matter volume to reading-related skills and history of dyslexia. Cereb Cortex 2010; 20: 2625–35.
Galaburda AM, Kemper TL. Cytoarchitectonic abnormalities in developmental dyslexia - case-study. Ann Neurol 1979; 6: 94–100.
Ge T, Feng J, Hibar DP, Thompson PM, Nichols TE. Increasing power for voxel-wise genome-wide association studies: the random field theory, least square kernel machines and fast permutation procedures. Neuroimage 2012; 63: 858–73.
Gilger JW, Hanebuth E, Smith SD, Pennington BF. Differential risk for developmental reading disorders in the offspring of compensated versus noncompensated parents. Read Writ 1996; 8: 407–17.
Hallgren B. Specific dyslexia (congenital word-blindness); a clinical and genetic study. Acta Psychiatr Neurol Suppl 1950; 65: 1–287.
Harlaar N, Spinath FM, Dale PS, Plomin R. Genetic influences on early word recognition abilities and disabilities: a study of 7-year-old twins. J Child Psychol Psychiatry 2005; 46: 373–84.
Heim S, Grande M. Fingerprints of developmental dyslexia. Trends Neurosci Educ 2012; 1: 10–14.
Hoeft F, Hernandez A, McMillon G, Taylor-Hill H, Martindale JL, Meyler A, et al. Neural basis of dyslexia: a comparison between dyslexic and nondyslexic children equated for reading ability. J Neurosci 2006; 26: 10700–8.
Hoeft F, Meyler A, Hernandez A, Juel C, Taylor-Hill H, Martindale JL, et al. Functional and morphometric brain dissociation between dyslexia and reading ability. Proc Natl Acad Sci USA 2007; 104: 4234–9.
Hosseini SM, Black JM, Soriano T, Bugescu N, Martinez R, Raman MM, et al. Topological properties of large-scale structural brain networks in children with familial risk for reading difficulties. Neuroimage 2013; 71: 260–74.
Im K, Raschle NM, Smith SA, Ellen Grant P, Gaab N. Atypical Sulcal Pattern in Children with Developmental Dyslexia and At-Risk Kindergarteners. Cereb Cortex 2016; 26: 1138–48.
Jednorog K, Marchewka A, Altarelli I, Lopez AKM, van Ermingen-Marbach M, Grande M, et al. How reliable are Gray matter disruptions in specific reading disability across multiple countries and languages? Insights from a Large-Scale Voxel-Based Morphometry Study. Human Brain Mapp 2015; 36: 1741–54.
Kaufman AS, Kaufman N, Melchers P, Preuß U. Kaufman assessment battery for children. Deutsche Version. Frankfurt: Swets & Zeitlinger; 2003.
Klingberg T, Hedehus M, Temple E, Salz T, Gabrieli JD, Moseley ME, et al. Microstructure of temporo-parietal white matter as a basis for reading ability: evidence from diffusion tensor magnetic resonance imaging. Neuron 2000; 25: 493–500.
Kraft I, Cafiero R, Schaadt G, Brauer J, Neef NE, Muller B, et al. Cortical differences in preliterate children at familiar risk of dyslexia are similar to those observed in dyslexic readers. Brain 2015; 138 (Pt 9): e378.
Langer N, Benjamin C, Minas J, Gaab N. The neural correlates of reading fluency deficits in children. Cereb Cortex 2015; 25: 1441–53.
Lehongre K, Ramus F, Villiermet N, Schwartz D, Giraud AL. Altered low-gamma sampling in auditory cortex accounts for the three main facets of dyslexia. Neuron 2011; 72: 1080–90.
Lenhard W, Schneider W. ELFE 1-6. Ein Leseverständnistest für Erst- bis Sechstklässler. Göttingen: Hogrefe; 2006.
Linkersdorfer J, Jurcoane A, Lindberg S, Kaiser J, Hasselhorn M, Fiebach CJ, et al. The association between gray matter volume and reading proficiency: a longitudinal study of beginning readers. J Cognitive Neurosci 2015; 27: 308–18.
Lyytinen H, Ahonen T, Eklund K, Guttorm T, Kulju P, Laakso ML, et al. Early development of children at familial risk for dyslexia-follow-up from birth to school age. Dyslexia 2004; 10: 146–78.
Marques JP, Kober T, Krueger G, van der Zwaag W, Van de Moortele PF, Gruetter R. MP2RAGE, a self bias-field corrected sequence for improved segmentation and T1-mapping at high field. Neuroimage 2010; 49: 1271–81.
Maurer U, Brem S, Bucher K, Kranz F, Benz R, Steinhausen HC, et al. Impaired tuning of a fast occipito-temporal response for print in dyslexic children learning to read. Brain 2007; 130 (Pt 12): 3200–10.
Maurer U, Bucher K, Brem S, Benz R, Kranz F, Schulz E, et al. Neurophysiology in preschool improves behavioral prediction of reading ability throughout primary school. Biol Psychiatry 2009; 66: 341–8.
Meda SA, Gelernter J, Gruen JR, Calhoun VD, Meng H, Cope NA, et al. Polymorphism of DCDC2 reveals differences in cortical morphology of healthy individuals-a preliminary voxel based morphometry study. Brain Imaging Behav 2008; 2: 21–6.
Menghini D, Hagberg GE, Caltagirone C, Petrosini L, Vicari S. Implicit learning deficits in dyslexic adults: an fMRI study. Neuroimage 2006; 33: 1218–26.
Menghini D, Hagberg GE, Petrosini L, Bozzali M, Macaluso E, Caltagirone C, et al. Structural correlates of implicit learning deficits in subjects with developmental dyslexia. Ann NY Acad Sci 2008; 1145: 212–21.
Moll K, Kunze S, Neuhoff N, Bruder J, Schulte-Korne G. Specific learning disorder: prevalence and gender differences. PLoS One 2014; 9: e103537.
Moll K, Landerl K. SLRT-II. Lese- und Rechtschreibtest. Weiterentwicklung des Salzburger Lese- und Rechtschreibtests (SLRT). Bern: Huber; 2010.
Monzalvo K, Fluss J, Billard C, Dehaene S, Dehaene-Lambertz G. Cortical networks for vision and language in dyslexic and normal children of variable socio-economic status. Neuroimage 2012; 61: 258–74.
Myers CA, Vandermosten M, Farris EA, Hancock R, Gimenez P, Black JM, et al. White matter morphometric changes uniquely predict children's reading acquisition. Psychol Sci 2014; 25: 1870–83.
Nicolson RI, Fawcett AJ, Berry EL, Jenkins IH, Dean P, Brooks DJ. Association of abnormal cerebellar activation with motor learning difficulties in dyslexic adults. Lancet 1999; 353: 1662–7.

Oldfield RC. The assessment and analysis of handedness: The Edinburgh inventory. Neuropsychologia 1971; 9: 97–113.
Paulesu E, Demonet JF, Fazio F, McCrory E, Chanoine V, Brunswick N, et al. Dyslexia: cultural diversity and biological unity. Science 2001; 291: 2165–7.
Penagarikano O, Abrahams BS, Herman EI, Winden KD, Gdalyahu A, Dong H, et al. Absence of CNTNAP2 leads to epilepsy, neuronal migration abnormalities, and core autism-related deficits. Cell 2011; 147: 235–46.
Peterson RL, Pennington BF. Developmental dyslexia. Lancet 2012; 379: 1997–2007.
Pinel P, Fauchereau F, Moreno A, Barbot A, Lathrop M, Zelenika D, et al. Genetic variants of FOXP2 and KIAA0319/TTRAP/THEM2 locus are associated with altered brain activation in distinct language-related regions. J Neurosci 2012; 32: 817–25.
Quinque D, Kittler R, Kayser M, Stoneking M, Nasidze I. Evaluation of saliva as a source of human DNA for population and association studies. Anal Biochem 2006; 353: 272–7.
Raschle NM, Chang M, Gaab N. Structural brain alterations associated with dyslexia predate reading onset. Neuroimage 2011; 57: 742–9.
Raschle NM, Zuk J, Gaab N. Functional characteristics of developmental dyslexia in left-hemispheric posterior brain regions predate reading onset. Proc Natl Acad Sci USA 2012; 109: 2156–61.
Rimrodt SL, Peterson DJ, Denckla MB, Kaufmann WE, Cutting LE. White matter microstructural differences linked to left perisylvian language network in children with dyslexia. Cortex 2010; 46: 739–49.
Rodenas-Cuadrado P, Ho J, Vernes SC. Shining a light on CNTNAP2: complex functions to complex disorders. Eur J Hum Genet 2014; 22: 171–8.
Schneider W, Schlagmüller M, Ennemoser M. Lesegeschwindigkeits- und -verständnistest für die Klassen 6-12 (LGVT 6-12). Göttingen: Hogrefe; 2007.
Schulte-Korne G. The prevention, diagnosis, and treatment of dyslexia. Dtsch Arztebl Int 2010; 107: 718–26; quiz 27.
Shaywitz SE, Shaywitz BA, Pugh KR, Fulbright RK, Constable RT, Mencl WE, et al. Functional disruption in the organization of the brain for reading in dyslexia. Proc Natl Acad Sci USA 1998; 95: 2636–41.
Silani G, Frith U, Demonet JF, Fazio F, Perani D, Price C, et al. Brain abnormalities underlying altered activation in dyslexia: a voxel based morphometry study. Brain 2005; 128 (Pt 10): 2453–61.
Skeide MA, Kirsten H, Kraft I, Schaadt G, Muller B, Neef N, et al. Genetic dyslexia risk variant is related to neural connectivity patterns underlying phonological awareness in children. Neuroimage 2015; 118: 414–21.
Stock C, Schneider W. DERET 1-2+. Deutscher Rechtschreibtest für das erste und zweite Schuljahr. Göttingen: Hogrefe; 2008a.
Stock C, Schneider W. DERET 3-4+. Deutscher Rechtschreibtest für das dritte und vierte Schuljahr. Göttingen: Hogrefe; 2008b.
Tanaka H, Black JM, Hulme C, Stanley LM, Kesler SR, Whitfield-Gabrieli S, et al. The brain basis of the phonological deficit in dyslexia is independent of IQ. Psychol Sci 2011; 22: 1442–51.
Thiebaut de Schotten M, Cohen L, Amemiya E, Braga LW, Dehaene S. Learning to read improves the structure of the arcuate fasciculus. Cereb Cortex 2014; 24: 989–95.
Threlkeld SW, McClure MM, Bai J, Wang Y, LoTurco JJ, Rosen GD, et al. Developmental disruptions and behavioral impairments in rats following in utero RNAi of Dyx1c1. Brain Res Bull 2007; 71: 508–14.
van der Leij A, van Bergen E, van Zuijen T, de Jong P, Maurits N, Maassen B. Precursors of developmental dyslexia: an overview of the longitudinal Dutch Dyslexia Programme study. Dyslexia 2013; 19: 191–213.
Vandermosten M, Boets B, Poelmans H, Sunaert S, Wouters J, Ghesquiere P. A tractography study in dyslexia: neuroanatomic correlates of orthographic, phonological and speech processing. Brain 2012; 135 (Pt 3): 935–48.
Verbeek E, Meuwissen ME, Verheijen FW, Govaert PP, Licht DJ, Kuo DS, et al. COL4A2 mutation associated with familial porencephaly and small-vessel disease. Eur J Hum Genet 2012; 20: 844–51.
Vernes SC, Oliver PL, Spiteri E, Lockstone HE, Puliyadi R, Taylor JM, et al. Foxp2 regulates gene networks implicated in neurite outgrowth in the developing brain. PLoS Genet 2011; 7: e1002145.
Wang GQ, Zhou YX, Gao Y, Chen H, Xia JG, Xu JQ, et al. Association of specific language impairment candidate genes CMIP and ATP2C2 with developmental dyslexia in Chinese population. J Neurolinguist 2015; 33: 163–71.
Wechsler D. Wechsler Preschool and Primary Scale of Intelligence (WPPSI-III). 3rd edn. Deutsche Version. Frankfurt: Pearson; 2009.
Wilcke A, Ligges C, Burkhardt J, Alexander M, Wolf C, Quente E, et al. Imaging genetics of FOXP2 in dyslexia. Eur J Hum Genet 2012; 20: 224–9.
Worsley KJ, Andermann M, Koulis T, MacDonald D, Evans AC. Detecting changes in nonisotropic images. Hum Brain Mapp 1999; 8: 98–101.
Yeatman JD, Dougherty RF, Ben-Shachar M, Wandell BA. Development of white matter and reading skills. Proc Natl Acad Sci USA 2012; 109: E3045–53.
Yue Y, Grossmann B, Galetzka D, Zechner U, Haaf T. Isolation and differential expression of two isoforms of the ROBO2/Robo2 axon guidance receptor gene in humans and mice. Genomics 2006; 88: 772–8.

NRSN1 associated grey matter volume of the visual word form area reveals dyslexia before school

Michael A. Skeide, Indra Kraft, Bent Müller, Gesa Schaadt, Nicole E. Neef, Jens Brauer, Arndt Wilcke, Holger Kirsten, Johannes Boltze, and Angela D. Friederici

Supplementary material

Psychometric data acquisition

General quality criteria. To provide a reliable literacy assessment after only one year of schooling, we made sure that all data analyzed in the present study were in accordance with three quality criteria. First, the participant must have been able to separately name all 26 letters of the core German alphabet. Second, the participant must have fully understood all tasks. Finally, the participant must have been alert, attentive and focused across the entire psychometric testing session.

Non-verbal IQ. In the total sample, non-verbal IQ data were not available for 7 participants who were therefore not included in the dyslexia case-control classification analysis. 11 individuals (one child MRI-scanned at age 5 and 10 children MRI-scanned at age 3) yielded a non-verbal IQ between 66 and 85. These children were excluded from the dyslexia classification analysis but not from the gene-brain association analysis since they reportedly did not suffer from neurological diseases or psychiatric disorders.

MR data acquisition

MRI was conducted on a 3.0-Tesla Siemens TIM Trio (Siemens AG) whole-body magnetic resonance scanner using a 12-radiofrequency-channel head coil. T1-weighted three-dimensional magnetization-prepared rapid-acquisition gradient echo (MP2RAGE) pulse sequences with TR = 5.000 ms, TE = 2.82 ms, TI_1 = 700 ms, TI_2 = 2.500 ms, FOV = 256 x 240, matrix size = 250 x 219 x 144 and voxel size = 1.3 x 1.3 x 1.3 mm^3 were acquired.

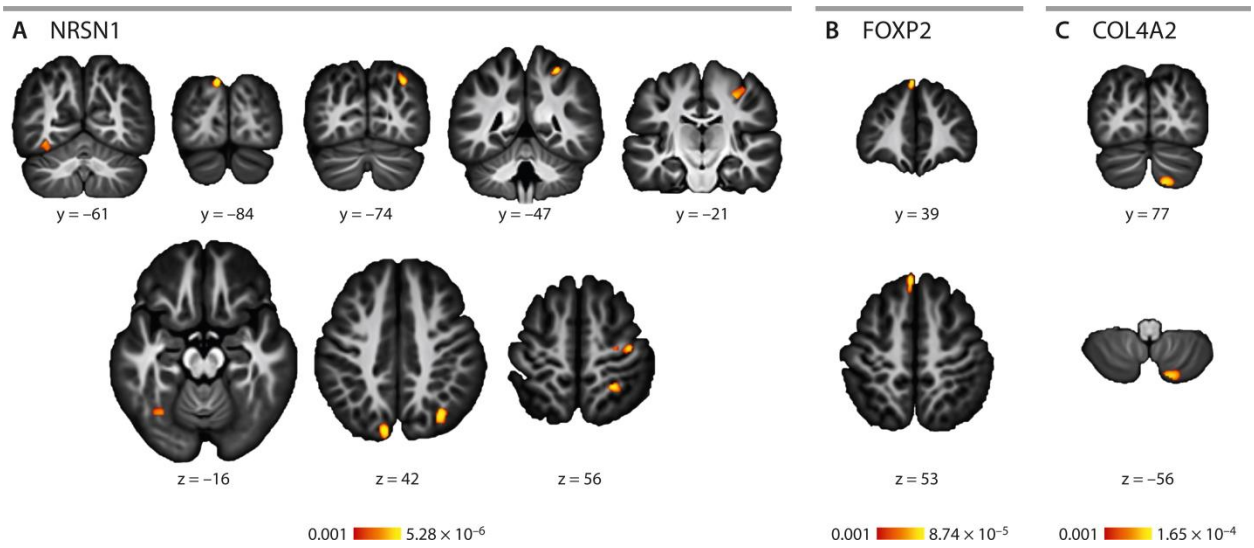

Figure S1 *P* value images showing all grey matter volume clusters that revealed a significant association with the genetic variants (A) NRSN1, (B) FOXP2, and (C) COL4A2. Y indicates the MNI coordinate of the coronal cut plane. Z indicates the MNI coordinate of the transversal cut plane. The color bar indicates the range of the corrected *p* values.

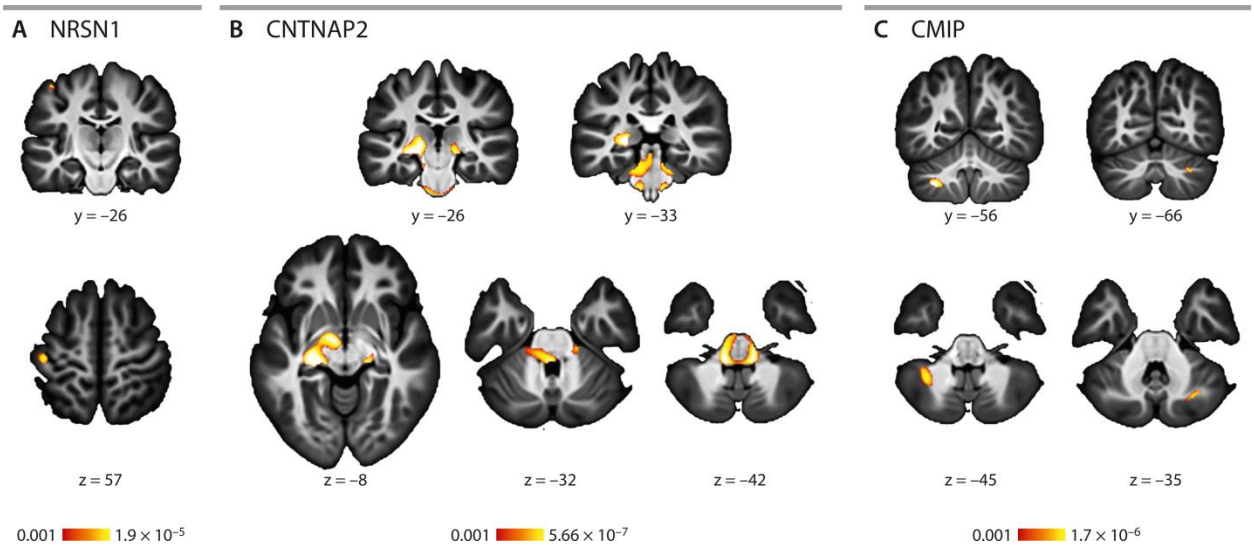

Figure S2 *P* value images showing all white matter volume clusters that revealed a significant association with the genetic variants (A) NRSN1, (B) CNTNAP2, and (C) CMIP. Y indicates the MNI coordinate of the coronal cut plane. Z indicates the MNI coordinate of the transversal cut plane. The color bar indicates the range of the corrected *p* values.

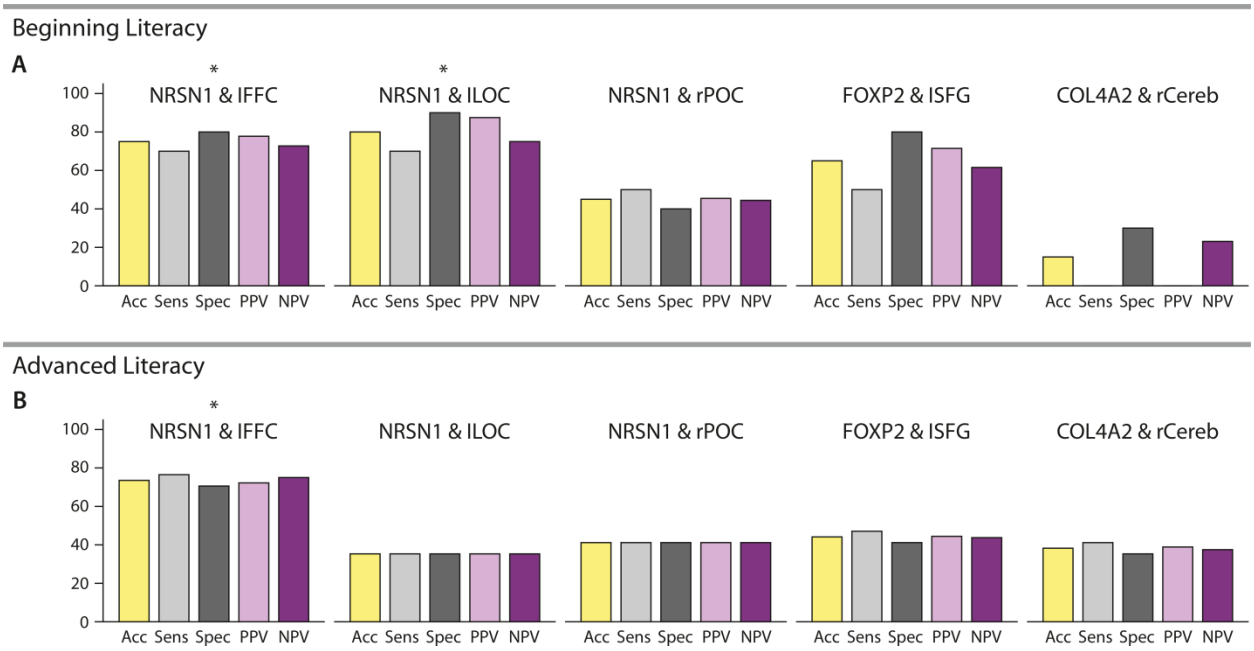

Figure S3 Classification indices for all 5 significant genetic associations with grey matter volume. **(A)** Beginning readers. Above-chance classification (marked by an asterisk) was revealed by the association between NRSN1 and the left lateral occipital cortex (p = 0.028, corrected) and by the association between NRSN1 and the left temporal occipital fusiform cortex (p = 0.035, corrected). **(B)** Advanced readers. Above-chance classification (marked by an asterisk) was revealed by the association between NRSN1 and the left temporal occipital fusiform cortex (p = 0.031, corrected). lFCC = left temporal occipital fusiform cortex, lLOC = left lateral occipital cortex, rPOC = right parieto-occipital cortex, lSFG = left superior frontal gyrus, rCereb = right cerebellum, VIIb, crus II, VIIIa. Five classification indices are displayed separately on the x-axis: Acc = Total Classification Accuracy (yellow), Sens = Sensitivity (light grey), Spec = Specificity (dark grey), PPV = Positive Predictive Value (light purple), NPV = Negative Predictive Value (dark purple). The y-axis displays the classification performance (0 to 100%).

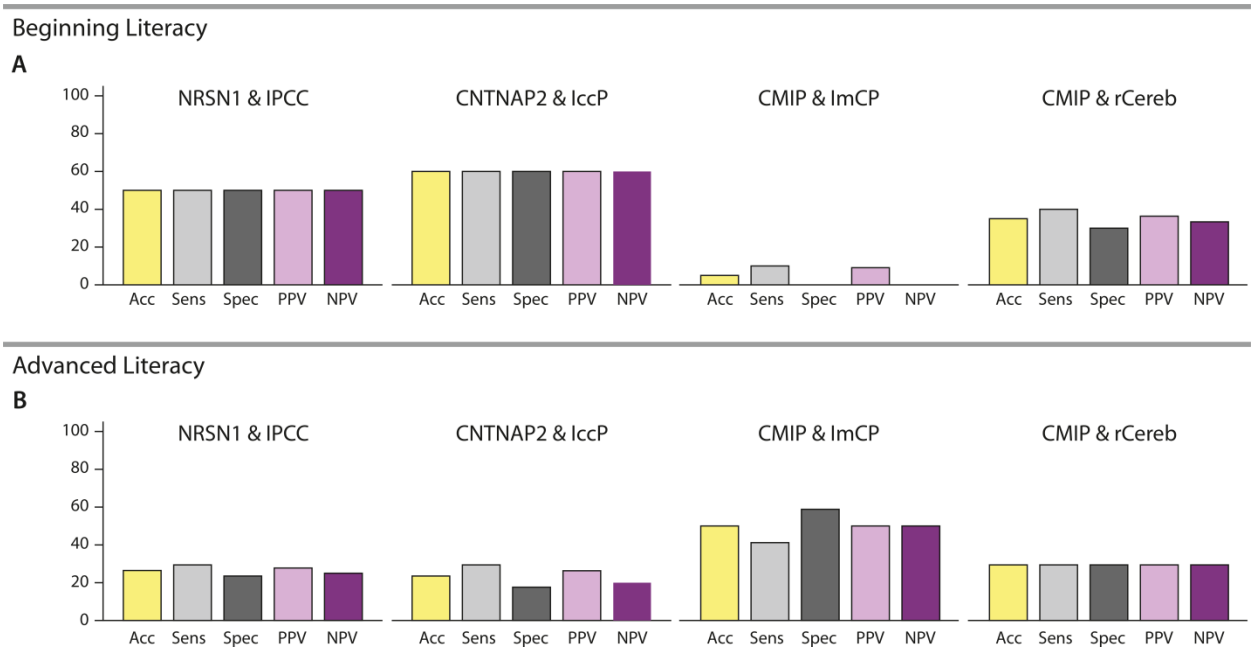

Figure S4 Classification indices for all 4 significant genetic associations with white matter volume. **(A)** Beginning readers. **(B)** Advanced readers. lPCC = local white matter of the left postcentral cortex, lccP = left cerebral / cerebellar peduncle, lmCP = left middle cerebellar peduncle, rCereb = local white matter of the right cerebellum, crus I (p =). Five classification indices are displayed separately on the x-axis: Acc = Total Classification Accuracy (yellow), Sens = Sensitivity (light grey), Spec = Specificity (dark grey), PPV = Positive Predictive Value (light purple), NPV = Negative Predictive Value (dark purple). The y-axis displays the classification performance (0 to 100%).

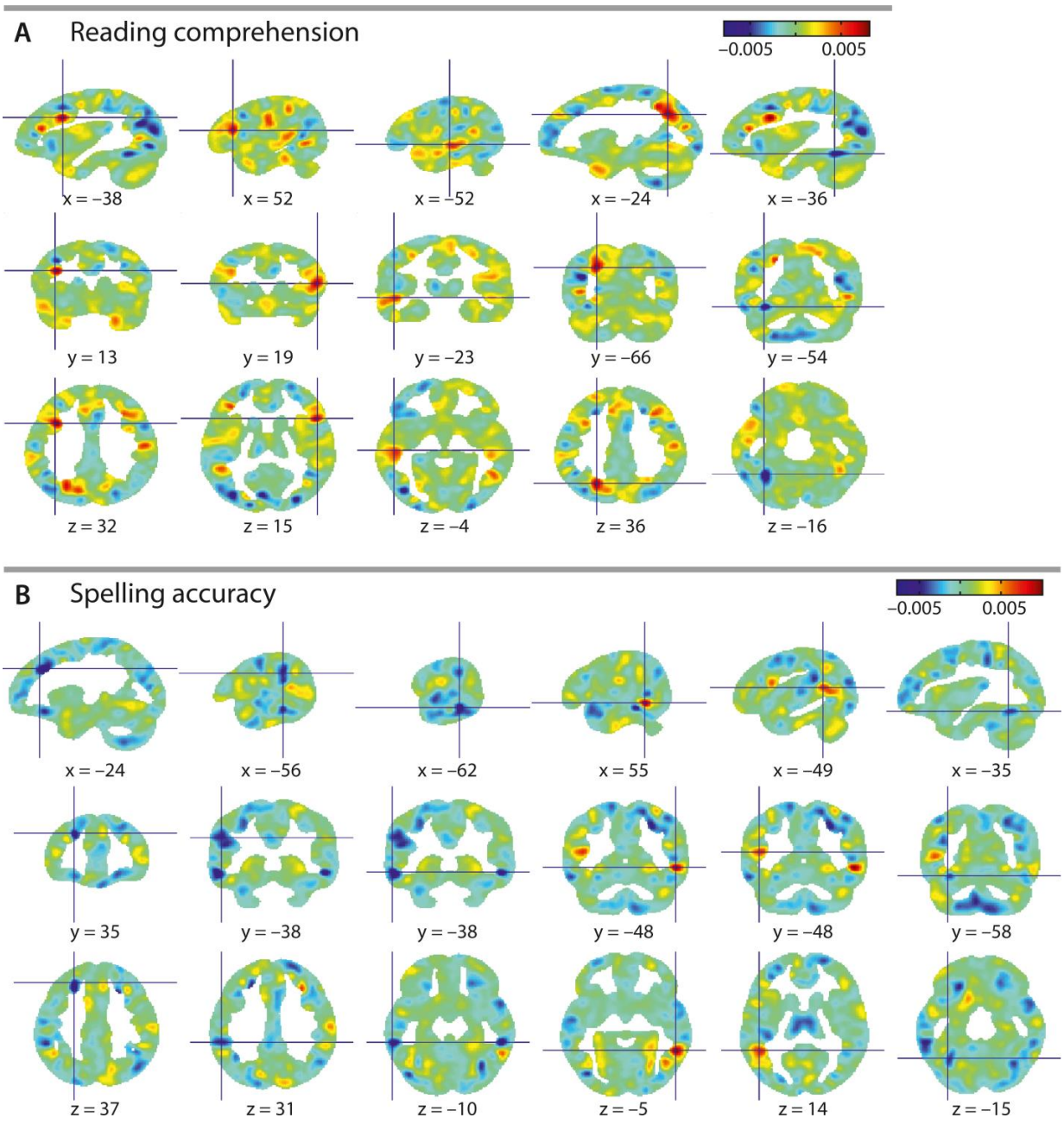

Figure S5 Non-significant whole-brain grey matter volume correlates of individual reading comprehension performance (R^2 = 0.03, p = 0.2916, corrected) **(A)** and individual spelling accuracy (R^2 = 0.05, p = 0.2715, corrected) **(B)**. Depicted are kernel ridge regression weight maps with cross-hairs over regions where weights exceeded the threshold of -0.005 (blue) or 0.005 (red). The color bar indicates the range of the regression weights. The letters x, y and z specify the MNI coordinates of the sagittal, coronal and transversal cut planes, respectively.

Table S1 (1/3) Characteristics of the Investigated Set of Single Nucleotide Polymorphisms

Chromosome	Nearest Gene[a]	SNP[b]	MAF[c]	*N* participants in Genotypic Groups[d]			Genotypic Groups		
				Hom Maj[e]	Hetero[f]	Hom Min[g]	Hom Maj[e]	Hetero[f]	Hom Min[g]
1	RCAN3 (Strippoli *et al.*, 2000)	rs196402 (Luciano *et al.*, 2013)	0.4610	39	74	28	GG	GA	AA
3	ROBO1 (Yue *et al.*, 2006)	rs162870 (Bates *et al.*, 2011)	0.3832	20	65	52	CC	AC	AA
3	ROBO1	rs331142 (Tran *et al.*, 2014)	0.2305	86	45	10	TT	GT	GG
3	ROBO1	rs12495133 (Tran *et al.*, 2014)	0.3830	57	60	24	CC	CA	AA
3	ROBO1	rs11127636 (Bates *et al.*, 2011)	0.4228	29	57	50	CC	AC	AA
3	ROBO1	rs4535189 (Bates *et al.*, 2011)	0.4679	43	63	34	TT	TC	CC
3	ROBO1	rs7614913 (Bates *et al.*, 2011)	0.4078	53	61	27	TT	TC	CC
3	ROBO1	rs6548628 (Bates *et al.*, 2011)	0.4787	34	67	40	CC	AC	AA
3	ROBO1	rs9853895 (Bates *et al.*, 2011)	0.4610	35	60	46	TT	CT	CC
3	ROBO1	rs1995402 (Bates *et al.*, 2011)	0.4220	49	65	27	CC	CA	AA
6	NRSN1 (Araki *et al.*, 2002)	rs9356928 (Couto *et al.*, 2010)	0.4965	35	72	34	GG	GA	AA
6	NRSN1	rs4285310 (Couto *et al.*, 2010)[h]	0.3321	62	63	15	TT	TG	GG
6	NRSN1	rs3178 (Couto *et al.*, 2010)	0.4894	40	64	37	TT	TC	CC
6	DCDC2 (Threlkeld *et al.*, 2007)	rs793842 (Darki *et al.*, 2012)	0.4149	53	59	29	GG	GA	AA
6	DCDC2	rs807701 (Schumacher *et al.*, 2006)	0.3830	56	62	23	TT	TC	CC
6	DCDC2	rs807724 (Meng *et al.*, 2005)	0.2376	82	51	8	AA	GA	GG
6	DCDC2	rs1091047 (Lind *et al.*, 2010)	0.2057	89	46	6	GG	CG	CC
6	DCDC2	rs6922023 (Lind *et al.*, 2010)	0.2057	10	38	93	AA	GA	GG
6	DCDC2	rs1087266 (Meng *et al.*, 2005)	0.4255	47	68	26	CC	CT	TT
6	KIAA0319 (Threlkeld *et al.*, 2007)	rs2179515 (Cope *et al.*, 2005)	0.4149	23	71	47	AA	GA	GG
6	KIAA0319	rs761100 (Harold *et al.*, 2006)	0.4858	36	73	32	GG	GT	TT
6	KIAA0319	rs6935076 (Harold *et al.*, 2006)	0.3333	62	64	15	CC	CT	TT
6	TDP2 (Gomez-Herreros *et al.*, 2014)	rs3181238 (Couto *et al.*, 2010)[i]	0.3022	67	60	12	GG	GA	AA
7	FOXP2 (Takahashi *et al.*, 2003)	rs923875 (Peter *et al.*, 2011)	0.4397	25	74	42	CC	CA	AA
7	FOXP2	rs12533005 (Peter *et al.*, 2011)	0.4362	27	69	45	CC	GC	GG
7	FOXP2	rs6980093 (Peter *et al.*, 2011)	0.3936	20	71	50	GG	GA	AA
7	FOXP2	rs10230558 (Peter *et al.*, 2011)	0.4468	38	80	23	AA	TA	TT
7	FOXP2	rs7782412 (Peter *et al.*, 2011)	0.4043	19	76	46	CC	TC	TT
7	FOXP2	rs936146 (Peter *et al.*, 2011)	0.4858	34	69	38	CC	GC	GG

[a] (reference for expression in brain tissue) [b] Single Nucleotide Polymorphism (reference for relation to literacy) [c] Minor Allele Frequency
[d] if $N \neq 141$, data are missing for the SNP (in ≥ 7 participants) [e] Homozygous Major Allele [f] Heterozygous [g] Homozygous Minor Allele
[h] replaced with proxy rs10946673 ($R^2 = 0.45$) [i] replaced with proxy rs2223588 ($R^2 = 0.83$)

Table S1 (2/3) Characteristics of the Investigated Set of Single Nucleotide Polymorphisms

Chromosome	Nearest Gene[a]	SNP[b]	MAF[c]	*N* participants in Genotypic Groups[d]			Genotypic Groups		
				Hom Maj[e]	Hetero[f]	Hom Min[g]	Hom Maj[e]	Hetero[f]	Hom Min[g]
7	DGKI	rs270891 (Matsson *et al.*, 2011)	0.4610	26	78	37	AA	CA	CC
7	DGKI	rs270904 (Matsson *et al.*, 2011)	0.3759	21	64	56	TT	TC	CC
7	DGKI	rs1991084 (Matsson *et al.*, 2011)	0.4043	25	64	52	GG	AG	AA
7	DGKI	rs889869 (Matsson *et al.*, 2011)	0.4752	32	70	39	AA	GA	GG
7	CREB3L2 (Sheng *et al.*, 2010)	rs273933 (Matsson *et al.*, 2011)	0.3333	19	56	66	AA	AG	GG
7	CNTNAP2 (Poliak *et al.*, 2001)	rs7794745 (Newbury *et al.*, 2011)	0.3617	56	68	17	AA	AT	TT
7	CNTNAP2	rs10246256 (Vernes *et al.*, 2008)	0.3582	21	59	61	CC	TC	TT
7	CNTNAP2	rs2710102 (Vernes *et al.*, 2008)	0.4894	41	62	38	TT	TC	CC
7	CNTNAP2	rs759178 (Vernes *et al.*, 2008)	0.4857	41	62	37	TT	GT	GG
7	CNTNAP2	rs17236239 (Vernes *et al.*, 2008)	0.2979	77	44	20	AA	AG	GG
7	CNTNAP2	rs4431523 (Vernes *et al.*, 2008)	0.3014	71	55	15	TT	CT	CC
7	CNTNAP2	rs2710117 (Vernes *et al.*, 2008)	0.4043	55	58	28	AA	AT	TT
13	COL4A2 (Verbeek *et al.*, 2012)	rs9521789 (Eicher *et al.*, 2013)	0.3794	52	71	18	TT	TC	CC
15	CYP19A1 (Coumailleau and Kah, 2014)	rs934634 (Anthoni *et al.*, 2012)	0.2234	7	49	85	TT	TC	CC
15	CYP19A1	rs10046 (Anthoni *et al.*, 2012)	0.4645	43	65	33	TT	CT	CC
15	CYP19A1	rs8034835 (Anthoni *et al.*, 2012)	0.4645	33	65	43	AA	AG	GG
15	DYX1C1-CCPG1 (Threlkeld *et al.*, 2007)	rs7174102 (Paracchini *et al.*, 2011)	0.3893	23	63	54	AA	AT	TT
15	DYX1C1-CCPG1	rs600753 (Dahdouh *et al.*, 2009)	0.4681	40	70	31	CC	CT	TT
15	DYX1C1-CCPG1	rs8037376 (Paracchini *et al.*, 2011)	0.3972	55	60	26	TT	TC	CC
15	DYX1C1-CCPG1	rs685935 (Bates *et al.*, 2010)	0.4433	45	67	29	TT	TC	CC
15	DYX1C1-CCPG1	rs11629841 (Wigg *et al.*, 2004)	0.4149	52	61	28	TT	GT	GG
15	DYX1C1-CCPG1	rs8043049 (Paracchini *et al.*, 2011)	0.4184	52	60	29	TT	CT	CC
15	DYX1C1-CCPG1	rs3743204 (Wigg *et al.*, 2004)	0.1489	6	30	105	TT	GT	GG
16	CMIP (Kato *et al.*, 2014)	rs12927866 (Wigg *et al.*, 2004)	0.3121	14	60	67	TT	CT	CC
16	CMIP	rs6564903 (Wigg *et al.*, 2004)	0.4113	23	70	48	TT	TC	CC
16	CMIP	rs3935802 (Wigg *et al.*, 2004)	0.3298	62	65	14	CC	GC	GG
16	CMIP	rs4265801 (Wigg *et al.*, 2004)	0.4291	26	69	46	GG	GT	TT
16	CMIP	rs16955705 (Scerri *et al.*, 2011)	0.3652	54	71	16	AA	CA	CC
16	CMIP	rs7201632 (Wigg *et al.*, 2004)	0.3759	19	68	54	CC	CT	TT

[a] (reference for expression in brain tissue) [b] Single Nucleotide Polymorphism (reference for relation to literacy) [c] Minor Allele Frequency
[d] if $N \neq 141$, data are missing for the SNP (in ≥ 7 participants) [e] Homozygous Major Allele [f] Heterozygous [g] Homozygous Minor Allele

Table S1 (3/3) Characteristics of the Investigated Set of Single Nucleotide Polymorphisms

Chromosome	Nearest Gene[a]	SNP[b]	MAF[c]	*N* participants in Genotypic Groups[d]			Genotypic Groups		
				Hom Maj[e]	Hetero[f]	Hom Min[g]	Hom Maj[e]	Hetero[f]	Hom Min[g]
16	ATP2C2 (Xiang *et al.*, 2005)	rs8053211 (Wigg *et al.*, 2004)	0.4929	41	57	43	GG	GA	AA
16	ATP2C2	rs11860694 (Wigg *et al.*, 2004)	0.4858	41	63	37	GG	GC	CC
16	ATP2C2	rs16973771 (Wigg *et al.*, 2004)	0.4149	27	63	51	CC	CT	TT
16	ATP2C2	rs2875891 (Wigg *et al.*, 2004)	0.3723	24	57	60	TT	CT	CC
16	ATP2C2	rs8045507 (Wigg *et al.*, 2004)	0.4078	26	63	52	AA	AG	GG
18	EPB41L3 (Martinez-Glez *et al.*, 2005)	rs11874896 (Scerri *et al.*, 2010)	0.1489	104	32	5	AA	TA	TT
18	DYM (El Ghouzzi *et al.*, 2003)	rs11873029 (Scerri *et al.*, 2010)	0.2057	89	46	6	CC	TC	TT
18	MYO5B (Rodriguez and Cheney, 2002)	rs555879 (Scerri *et al.*, 2010)	0.4716	38	73	30	TT	CT	CC
18	NEDD4L (Dergham *et al.*, 2007)	rs8094327 (Scerri *et al.*, 2010)	0.1738	100	33	8	AA	GA	GG
18	NEDD4L	rs12606138 (Scerri *et al.*, 2010)	0.1667	7	33	101	GG	AG	AA

[a] (reference for expression in brain tissue) [b] Single Nucleotide Polymorphism (reference for relation to literacy) [c] Minor Allele Frequency
[d] if $N \neq 141$, data are missing for the SNP (in ≥ 7 participants) [e] Homozygous Major Allele [f] Heterozygous [g] Homozygous Minor Allele

Table S2 (1/2) Age of MRI data acquisition, age of psychometric data acquisition and time between MRI data acquisition and psychometric data acquisition

Participant	Dyslexia	T_{MRI} [a]	T_{Psych} [b]	Δ [c]
1	no	12.17	13.67	1.50
2	no	11.58	13.58	2.00
3	no	11.50	13.58	2.08
4	yes	11.42	13.50	2.08
5	no	11.25	11.25	0
6	no	11.25	11.25	0
7	yes	11.17	13.50	2.33
8	no	11.17	13.17	2.00
9	yes	11.08	13.50	2.42
10	yes	11.00	11.33	0.33
11	no	10.92	12.92	2.00
12	no	10.92	13.08	2.16
13	yes	10.83	13.42	2.59
14	yes	10.75	11.00	0.25
15	yes	10.75	13.08	2.33
16	yes	10.67	11.00	0.33
17	no	10.58	12.92	2.34
18	yes	10.50	10.83	0.33
19	no	10.33	12.50	2.17
20	no	10.33	12.75	2.42
21	yes	10.25	12.42	2.17
22	yes	10.17	10.17	0
23	yes	10.08	12.75	2.67
24	yes	10.08	12.42	2.34
25	yes	10.00	10.00	0
26	no	9.92	12.50	2.58
27	yes	9.92	12.50	2.58
28	no	9.92	12.00	2.08
29	no	9.83	12.17	2.34
30	no	9.75	12.25	2.50

[a] Age (in years) of MRI data acquisition
[b] Age (in years) of psychometric data acquisition
[c] Time (in years) between MRI data acquisition and psychometric data acquisition

The time between MRI data acquisition and psychometric data acquisition did not differ significantly between dyslexic and control individuals:
34 participants that underwent MRI between 9 and 12 years of age: $z = 0.24$, $p = 0.812$
20 participants that underwent MRI between 5 and 6 years of age: $F = 0.066$, $p = 0.800$
combined sample of 54 participants: $z = 0.48$, $p = 0.634$

Table S2 (2/2) Age of MRI data acquisition, age of psychometric data acquisition and time between MRI data acquisition and psychometric data acquisition

Participant	Dyslexia	T_{MRI} [a]	T_{Psych} [b]	Δ [c]
31	no	9.75	12.17	2.42
32	yes	9.50	10.08	0.58
33	yes	9.42	12.08	2.66
34	no	9.17	11.92	2.75
35	yes	6.33	7.92	1.59
36	no	6.08	7.67	1.59
37	no	6.08	8.58	2.50
38	yes	6.00	8.08	2.08
39	yes	5.92	7.67	1.75
40	yes	5.92	7.92	2.00
41	no	5.92	7.17	1.25
42	no	5.92	8.25	2.33
43	no	5.83	7.58	1.75
44	no	5.83	7.58	1.75
45	no	5.83	7.75	1.92
46	no	5.75	7.33	1.58
47	yes	5.58	7.08	1.50
48	no	5.50	7.92	2.42
49	no	5.42	7.75	2.33
50	yes	5.33	7.50	2.17
51	yes	5.25	7.25	2.00
52	yes	5.25	7.75	2.50
53	yes	5.17	7.33	2.16
54	yes	5.08	7.17	2.09

[a] Age of MRI data acquisition
[b] Age of psychometric data acquisition
[c] Time between MRI data acquisition and psychometric data acquisition

The time between MRI data acquisition and psychometric data acquisition did not differ significantly between dyslexic and control individuals:
34 participants that underwent MRI between 9 and 12 years of age: $z = 0.24$, $p = 0.812$
20 participants that underwent MRI between 5 and 6 years of age: $F = 0.066$, $p = 0.800$
combined sample of 54 participants: $z = 0.48$, $p = 0.634$

Table S3 Anatomical labels, sizes, MNI coordinates and *p* values of all grey matter volume clusters that were significantly associated with (a) NRSN1, (b) FOXP2, and (c) COL4A2

a (NRSN1)

		MNI Coordinates			
Macroanatomical Region[a]	**Cluster Size**[c]	**x**	**y**	**z**	$p_{VoxelMax}$[d]
Right Pre- and Postcentral Gyri[b]	255	42	-18	53	9.92×10^{-5}
Right Lateral Occipital Cortex, Superior Division[b]	224	35	-71	41	2.88×10^{-5}
Right Superior Parietal Lobule[b]	102	29	-48	57	5.40×10^{-5}
Left Lateral Occipital Cortex	147	-9	-83	42	5.28×10^{-6}
Left Temporal Occipital Fusiform Cortex	100	-33	-63	-18	3.19×10^{-4}

b (FOXP2)

		MNI Coordinates			
Macroanatomical Region[a]	**Cluster Size**[c]	**x**	**y**	**z**	$p_{VoxelMax}$[d]
Left Superior Frontal Gyrus	185	-3	38	53	8.74×10^{-5}

c (COL4A2)

		MNI Coordinates			
Macroanatomical Region[e]	**Cluster Size**[c]	**x**	**y**	**z**	$p_{VoxelMax}$[d]
Right Cerebellum, VIIb, Crus II, VIIIa	270	17	-77	-54	1.65×10^{-4}

[a] according to the Harvard-Oxford Cortical Structural Atlas
[b] these sub-clusters form a continuous cluster at $p < 0.001$before further correcting for size and number of genes
[c] corrected *n* voxels
[d] corrected *p* value of the most significant voxel within the cluster
[e] according to the Cerebellar Atlas

Table S4 Anatomical labels, sizes, MNI coordinates and *p* values of all white matter volume clusters that were significantly associated with (a) NRSN1, (b) CNTNAP2, and (c) CMIP

a (NRSN1)

		MNI Coordinates			
Macroanatomical Region	**Cluster Size**[c]	**x**	**y**	**z**	$p_{VoxelMax}$[d]
Local White Matter of the Left Postcentral Cortex	58	-45	-23	60	1.90×10^{-5}

b (CNTNAP2)

		MNI Coordinates			
Macroanatomical Region[a]	**Cluster Size**[c]	**x**	**y**	**z**	$p_{VoxelMax}$[d]
Left Cerebral Peduncle[b]	2.172	-20	-27	-8	5.66×10^{-7}
Left Inferior Cerebellar Peduncle[b]	1.718	-11	-41	-45	1.70×10^{-6}

c (CMIP)

		MNI Coordinates			
Macroanatomical Region	**Cluster Size**[c]	**x**	**y**	**z**	$p_{VoxelMax}$[d]
Left Middle Cerebellar Peduncle	288	-9	-83	42	1.70×10^{-6}
Local White Matter of the Right Cerebellum, Crus I	63	32	-68	-36	6.86×10^{-5}

[a] according to the Johns Hopkins University ICBM-DTI-81 White Matter Atlas
[b] these sub-clusters form a continuous cluster at $p < 0.001$before further correcting for size and number of genes
[c] corrected *n* voxels
[d] corrected *p* value of the most significant voxel within the cluster

Table S5 Associations between dyslexia candidate genes and literacy skills

Gene	Reading comprehension	Reading speed	Spelling accuracy
RCAN3	$\chi(1) =$ 0.41, $p = 0.520$	$\chi(1) = 0.46$, $p = 0.498$	$\chi(1) = 0.45$, $p = 0.503$
ROBO1	$\chi(9) = 10.92$, $p = 0.282$	$\chi(9) = 10.06$, $p = 0.345$	$\chi(9) = 3.35$, $p = 0.949$
NRSN1	**$\chi(3) = 14.54$, $p = 0.002$***	$\chi(3) = 7.22$, $p = 0.065$	$\chi(3) = 5.20$, $p = 0.158$
DCDC2	$\chi(6) = 11.33$, $p = 0.079$	$\chi(6) = 3.07$, $p = 0.800$	$\chi(6) = 7.67$, $p = 0.264$
KIAA0319	**$\chi(3) = 7.86$, $p = 0.049$**	**$\chi(3) = 9.77$, $p = 0.021$**	$\chi(3) = 0.98$, $p = 0.806$
TDP2	$\chi(1) = 2.04$, $p = 0.153$	**$\chi(1) = 4.378$, $p = 0.036$**	$\chi(1) = 0.42$, $p = 0.516$
FOXP2	$\chi(6) = 8.60$, $p = 0.198$	$\chi(6) = 12.17$, $p = 0.058$	$\chi(6) = 12.36$, $p = 0.054$
DGKI	$\chi(4) = 5.21$, $p = 0.266$	$\chi(4) = 3.55$, $p = 0.471$	$\chi(4) = 1.54$, $p = 0.819$
CREB3L2	$\chi(1) = 0.22$, $p = 0.636$	$\chi(1) = 0.27$, $p = 0.604$	$\chi(1) = 0.60$, $p = 0.440$
CNTNAP2	**$\chi(6) = 13.77$, $p = 0.032$**	$\chi(6) = 4.17$, $p = 0.654$	$\chi(6) = 7.36$, $p = 0.289$
COL4A2	$\chi(1) = 0.14$, $p = 0.711$	$\chi(1) = 0.01$, $p = 0.928$	$\chi(1) = 0.16$, $p = 0.686$
CYP19A1	$\chi(2) = 1.86$, $p = 0.395$	$\chi(2) = 0.97$, $p = 0.617$	$\chi(2) = 5.30$, $p = 0.071$
DYX1C1-CCPG1	$\chi(6) = 4.09$, $p = 0.665$	$\chi(6) = 3.68$, $p = 0.720$	$\chi(6) = 5.41$, $p = 0.492$
CMIP	**$\chi(5) = 18.69$, $p = 0.002$***	$\chi(5) = 8.57$, $p = 0.127$	$\chi(5) = 4.77$, $p = 0.664$
ATP2C2	$\chi(4) = 0.52$, $p = 0.972$	$\chi(4) = 3.46$, $p = 0.484$	$\chi(4) = 8.09$, $p = 0.088$
EPB41L3	$\chi(1) = 0.80$, $p = 0.371$	$\chi(1) = 2.29$, $p = 0.131$	$\chi(1) = 2.43$, $p = 0.119$
DYM	$\chi(1) = 0$, $p = 0.990$	$\chi(1) = 0.62$, $p = 0.430$	$\chi(1) = 0.34$, $p = 0.562$
MYO5B	$\chi(1) = 0.33$, $p = 0.566$	$\chi(1) = 0.09$, $p = 0.760$	$\chi(1) = 0.83$, $p = 0.361$
NEDD4L	$\chi(2) = 2.62$, $p = 0.270$	$\chi(2) = 4.35$, $p = 0.114$	$\chi(2) = 2.33$, $p = 0.311$

* $p < 0.05$ after family-wise error correction

Supplementary references

Anthoni H, Sucheston LE, Lewis BA, Tapia-Paez I, Fan X, Zucchelli M, *et al.* The aromatase gene CYP19A1: several genetic and functional lines of evidence supporting a role in reading, speech and language. Behav Genet 2012; 42(4): 509-27.

Araki M, Nagata K, Satoh Y, Kadota Y, Hisha H, Adachi Y, *et al.* Developmentally regulated expression of Neuro-p24 and its possible function in neurite extension. Neurosci Res 2002; 44(4): 379-89.

Bates TC, Lind PA, Luciano M, Montgomery GW, Martin NG, Wright MJ. Dyslexia and DYX1C1: deficits in reading and spelling associated with a missense mutation. Mol Psychiatry 2010; 15(12): 1190-6.

Bates TC, Luciano M, Medland SE, Montgomery GW, Wright MJ, Martin NG. Genetic variance in a component of the language acquisition device: ROBO1 polymorphisms associated with phonological buffer deficits. Behav Genet 2011; 41(1): 50-7.

Cope N, Harold D, Hill G, Moskvina V, Stevenson J, Holmans P, *et al.* Strong evidence that KIAA0319 on chromosome 6p is a susceptibility gene for developmental dyslexia. Am J Hum Genet 2005; 76(4): 581-91.

Coumailleau P, Kah O. Cyp19a1 (Aromatase) Expression in the Xenopus Brain at Different Developmental Stages. J Neuroendocrinol 2014; 26(4): 226-36.

Couto JM, Livne-Bar I, Huang K, Xu Z, Cate-Carter T, Feng Y, *et al.* Association of reading disabilities with regions marked by acetylated H3 histones in KIAA0319. Am J Med Genet B Neuropsychiatr Genet 2010; 153B(2): 447-62.

Dahdouh F, Anthoni H, Tapia-Paez I, Peyrard-Janvid M, Schulte-Korne G, Warnke A, *et al.* Further evidence for DYX1C1 as a susceptibility factor for dyslexia. Psychiatr Genet 2009; 19(2): 59-63.

Darki F, Peyrard-Janvid M, Matsson H, Kere J, Klingberg T. Three dyslexia susceptibility genes, DYX1C1, DCDC2, and KIAA0319, affect temporo-parietal white matter structure. Biol Psychiatry 2012; 72(8): 671-6.

Dergham EE, Wang HW, Tesson F, Leenen F. Expression of Nedd4L gene in brain of Dahl rats. Faseb J 2007; 21(6): A1407-A8.

Eicher JD, Powers NR, Miller LL, Akshoomoff N, Amaral DG, Bloss CS, *et al.* Genome-wide association study of shared components of reading disability and language impairment. Genes Brain Behav 2013; 12(8): 792-801.

El Ghouzzi V, Dagoneau N, Kinning E, Thauvin-Robinet C, Chemaitilly W, Prost-Squarcioni C, *et al.* Mutations in a novel gene Dymeclin (FLJ20071) are responsible for Dyggve-Melchior-Clausen syndrome. Hum Mol Genet 2003; 12(3): 357-64.

Gomez-Herreros F, Schuurs-Hoeijmakers JH, McCormack M, Greally MT, Rulten S, Romero-Granados R, *et al.* TDP2 protects transcription from abortive topoisomerase activity and is required for normal neural function. Nat Genet 2014; 46(5): 516-21.

Harold D, Paracchini S, Scerri T, Dennis M, Cope N, Hill G, *et al.* Further evidence that the KIAA0319 gene confers susceptibility to developmental dyslexia. Mol Psychiatry 2006; 11(12): 1085-91, 61.

Kato M, Okanoya K, Koike T, Sasaki E, Okano H, Watanabe S, *et al.* Human speech- and reading-related genes display partially overlapping expression patterns in the marmoset brain. Brain Lang 2014; 133: 26-38.

Lind PA, Luciano M, Wright MJ, Montgomery GW, Martin NG, Bates TC. Dyslexia and DCDC2: normal variation in reading and spelling is associated with DCDC2 polymorphisms in an Australian population sample. Eur J Hum Genet 2010; 18(6): 668-73.

Luciano M, Evans DM, Hansell NK, Medland SE, Montgomery GW, Martin NG, *et al.* A genome-wide association study for reading and language abilities in two population cohorts. Genes Brain Behav 2013; 12(6): 645-52.

Martinez-Glez V, Bello MJ, Franco-Hernandez C, De Campos JM, Isla A, Vaquero J, *et al.* Mutational analysis of the DAL-1/4.1B tumour-suppressor gene locus in meningiomas. Int J Mol Med 2005; 16(4): 771-4.

Matsson H, Tammimies K, Zucchelli M, Anthoni H, Onkamo P, Nopola-Hemmi J, *et al.* SNP variations in the 7q33 region containing DGKI are associated with dyslexia in the Finnish and German populations. Behav Genet 2011; 41(1): 134-40.

Meng H, Smith SD, Hager K, Held M, Liu J, Olson RK, *et al.* DCDC2 is associated with reading disability and modulates neuronal development in the brain. Proc Natl Acad Sci U S A 2005; 102(47): 17053-8.

Newbury DF, Paracchini S, Scerri TS, Winchester L, Addis L, Richardson AJ, *et al.* Investigation of dyslexia and SLI risk variants in reading- and language-impaired subjects. Behav Genet 2011; 41(1): 90-104.

Paracchini S, Ang QW, Stanley FJ, Monaco AP, Pennell CE, Whitehouse AJ. Analysis of dyslexia candidate genes in the Raine cohort representing the general Australian population. Genes Brain Behav 2011; 10(2): 158-65.

Peter B, Raskind WH, Matsushita M, Lisowski M, Vu T, Berninger VW, *et al.* Replication of CNTNAP2 association with nonword repetition and support for FOXP2 association with timed reading and motor activities in a dyslexia family sample. J Neurodev Disord 2011; 3(1): 39-49.

Poliak S, Gollan L, Salomon D, Berglund EO, Ohara R, Ranscht B, *et al.* Localization of Caspr2 in myelinated nerves depends on axon-glia interactions and the generation of barriers along the axon. J Neurosci 2001; 21(19): 7568-75.

Rodriguez OC, Cheney RE. Human myosin-Vc is a novel class V myosin expressed in epithelial cells. J Cell Sci 2002; 115(5): 991-1004.

Scerri TS, Morris AP, Buckingham LL, Newbury DF, Miller LL, Monaco AP, *et al.* DCDC2, KIAA0319 and CMIP are associated with reading-related traits. Biol Psychiatry 2011; 70(3): 237-45.

Scerri TS, Paracchini S, Morris A, MacPhie IL, Talcott J, Stein J, *et al.* Identification of candidate genes for dyslexia susceptibility on chromosome 18. PLoS One 2010; 5(10): e13712.

Schumacher J, Anthoni H, Dahdouh F, Konig IR, Hillmer AM, Kluck N, *et al.* Strong genetic evidence of DCDC2 as a susceptibility gene for dyslexia. Am J Hum Genet 2006; 78(1): 52-62.

Sheng Z, Li L, Zhu LJ, Smith TW, Demers A, Ross AH, *et al.* A genome-wide RNA interference screen reveals an essential CREB3L2-ATF5-MCL1 survival pathway in malignant glioma with therapeutic implications. Nat Med 2010; 16(6): 671-7.

Strippoli P, Lenzi L, Petrini M, Carinci P, Zannotti M. A new gene family including DSCR1 (Down Syndrome Candidate Region 1) and ZAKI-4: characterization from yeast to human and identification of DSCR1-like 2, a novel human member (DSCR1L2). Genomics 2000; 64(3): 252-63.

Takahashi K, Liu FC, Hirokawa K, Takahashi H. Expression of Foxp2, a gene involved in speech and language, in the developing and adult striatum. J Neurosci Res 2003; 73(1): 61-72.

Threlkeld SW, McClure MM, Bai J, Wang Y, LoTurco JJ, Rosen GD, *et al.* Developmental disruptions and behavioral impairments in rats following in utero RNAi of Dyx1c1. Brain Res Bull 2007; 71(5): 508-14.

Tran C, Wigg KG, Zhang K, Cate-Carter TD, Kerr E, Field LL, *et al.* Association of the ROBO1 gene with reading disabilities in a family-based analysis. Genes Brain Behav 2014; 13(4): 430-8.

Verbeek E, Meuwissen ME, Verheijen FW, Govaert PP, Licht DJ, Kuo DS, *et al.* COL4A2 mutation associated with familial porencephaly and small-vessel disease. Eur J Hum Genet 2012; 20(8): 844-51.

Vernes SC, Newbury DF, Abrahams BS, Winchester L, Nicod J, Groszer M, *et al.* A functional genetic link between distinct developmental language disorders. N Engl J Med 2008; 359(22): 2337-45.

Wigg KG, Couto JM, Feng Y, Anderson B, Cate-Carter TD, Macciardi F, *et al.* Support for EKN1 as the susceptibility locus for dyslexia on 15q21. Mol Psychiatry 2004; 9(12): 1111-21.

Xiang MH, Mohamalawari D, Rao R. A novel isoform of the secretory pathway Ca2+, Mn2+-ATPase, hSPCA2, has unusual properties and is expressed in the brain. J Biol Chem 2005; 280(12): 11608-14.

Yue Y, Grossmann B, Galetzka D, Zechner U, Haaf T. Isolation and differential expression of two isoforms of the ROBO2/Robo2 axon guidance receptor gene in humans and mice. Genomics 2006; 88(6): 772-8.